


Research Article

Paleomagnetic data from volcanic rocks in the southern Central Andes of Argentina and their implications for tectonics and geomagnetic field behavior

M.L. Perez^{a,b} , F.N. Milanese^{b,c}, S.E. Geuna^{b,d}, P.R. Franceschinis^{a,b}, C. Puigdomenech^c, A. Folguera^{b,e} and A.E. Rapalini^{a,b}

^aUniversidad de Buenos Aires, Instituto de Geociencias Básicas, Aplicadas y Ambientales de Buenos Aires (IGEBA), CONICET, Buenos Aires, CP 1428, Argentina; ^bConsejo Nacional de Investigaciones Científicas y Técnicas (CONICET) Buenos Aires, CP 1425, Argentina; ^cInstituto Antártico Argentino (IAA), San Martín, CP 1650, Argentina; ^dInstituto de Bio y Geociencias del NOA (IBIGEO), Universidad Nacional de Salta, CONICET, Salta, CP 4405, Argentina and ^eInstituto de Estudios Andinos “Don Pablo Groeber” (IDEAN)–(UBA-CONICET), Buenos Aires, CP 1428, Argentina

Abstract

A paleomagnetic study of basaltic lava flows exposed in the northern Neuquén Cordillera, southernmost Central Andes, along the Antifir-Copahue fault zone (ACFZ), involved 25 sites of the Cola de Zorro Formation (Pliocene–Early Pleistocene) along two different sections. The sites show exclusive normal polarity, corresponding to the Late Pliocene Gauss chron (3.6–2.6 Ma). The angular standard deviation of virtual geomagnetic poles (VGPs; ASD = 14.8°) is consistent with the expected values from recent geomagnetic models, in opposition to anomalously low dispersion found in previous studies in Pleistocene VGPs of reverse polarity from neighboring areas to our study zone. Mean paleomagnetic directions for Bella Vista (Dec = 0.0°, Inc = –50.0°, α_{95} = 7.6°, K = 36.7, N = 11) and Río Huaraco sections (Dec = 354.9°, Inc = –57.0°, α_{95} = 7.5°, K = 55.7, N = 8) do not show tectonic rotation around vertical axes. Combining and regrouping our and previous data by area confirmed the absence of tectonic rotations in the Huaraco-Trohunco block and a statistically significant clockwise rotation of 14.4° ± 10.3° of three adjacent tectonic blocks located south of our study locality in Pleistocene times. These results suggest that strike-slip deformation along some sections of the ACFZ was significant in the Pleistocene structural evolution of this region.

Keywords: Tectonic rotations, Cola de Zorro Formation, Pleistocene, Liquiñe-Ofqui

(Received 26 December 2023; accepted 30 October 2024)

INTRODUCTION

The northern sector of the Neuquén Cordillera (~36.5°S–38°S) corresponds to a transition zone between the southern Central Andes and the North Patagonian Andes (Fig. 1). Its Neogene tectonic activity has been determined by the presence of the Guañacos fold and thrust belt (Folguera et al., 2006), located in the retroarc, and active since the Late Miocene. This fold and thrust belt presents evidence of neotectonic activity with dextral transpressive and transtensive deformation along the complex Antifir-Copahue Fault System (ACFS; Folguera et al., 2004; Colavitto et al., 2020; Fig. 2).

Folguera et al. (2004) showed that the ACFS constitutes the eastern orogenic front of the Andes in this region and is interpreted as the northernmost extension of the dextral strike-slip Liquiñe-Ofqui Fault Zone (LOFZ; Figs. 1 and 2). It has been active during the Pliocene and Pleistocene, since eastward migration of the front at the end of the Miocene. From then on, tectonic

shortening occurred in the easternmost areas of the Guañacos fold and thrust belt directly associated with the ACFS activity. Deformation in the region did not progress farther east of the major high-angle west-verging Trocomán-Nahueve Rivers thrust faults (Fig. 2).

Throughout the 90–100 km length of the ACFS, three sections are distinguished (Fig. 2). The northern section (NACFS) exposes NW-trending dextral transpressive structures, the central section (CACFS) is characterized by N-trending dextral transtensional structures and subordinate transpressive faults, and the southern section (SACFS) corresponds to a complex zone with NE-trending dextral oblique reverse faults and a series of transfer faults between the ACFS and the northern LOFZ. The LOFZ is a 1100-km-long strike-slip fault zone that accommodates the oblique convergence between the Nazca and South American plates and dominates the present tectonics and volcanism in the Andean arc, between 38°S and 48°S (Cembrano et al., 2000; Cembrano and Lara, 2009). This system has been active from the Neogene (Cembrano and Hervé, 1993), displaying present-day seismic activity (Lange et al., 2008).

Paleomagnetic studies carried out along the LOFZ reported tectonic rotations around vertical axes from ~44.3°S to 37.7°S (García et al., 1988; Cembrano et al., 1992; Rojas et al., 1994;

Corresponding author: M. L. Perez; Email: mperez@gl.fcen.uba.ar

Cite this article: Perez ML, Milanese FN, Geuna SE, Franceschinis PR, Puigdomenech C, Folguera A, Rapalini AE (2025). Paleomagnetic data from volcanic rocks in the southern Central Andes of Argentina and their implications for tectonics and geomagnetic field behavior. *Quaternary Research* 1–18. <https://doi.org/10.1017/qua.2024.52>



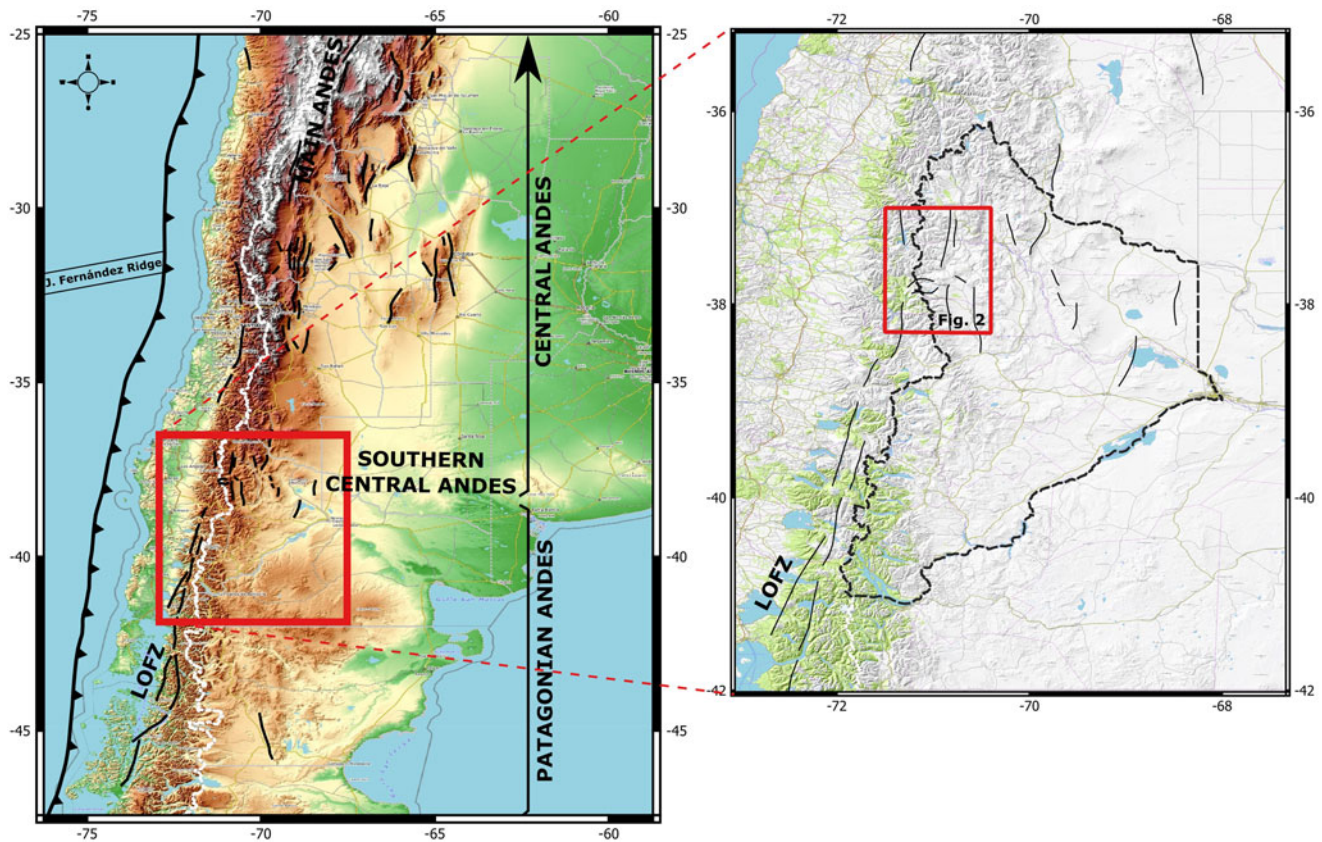


Figure 1. Location of the study area and regional tectonic setting based on Cembrano et al. (1996) and Sagripanti et al. (2018). Black solid lines indicate traces of Quaternary structures. LOFZ, Liquiñe-Ofqui Fault Zone.

Beck et al., 2000; Hernandez-Moreno et al., 2014, 2016; Siravo et al., 2020). A pattern of large magnitude and complex tectonic rotations in Chilean territory, along the northern areas of the LOFZ, was recently proposed (Hernandez-Moreno et al., 2014, 2016; Siravo et al., 2020). However, Milanese et al. (2023) cast doubts on the statistical validity of such results. They also proposed that possible tectonic rotations in the NACFS should be further investigated based on their paleomagnetic study on Plio-Pleistocene lavas near the Andacollo locality (Fig. 2), that yielded clockwise rotation values of $8.1^\circ \pm 8.4^\circ$, marginally insignificant at 95% confidence. Furthermore, preliminary results obtained from Miocene volcanic rocks exposed at the El Moncol locality (Fig. 2) suggest a $25.1^\circ \pm 18.3^\circ$ clockwise rotation (Escosteguy et al., 1999; Milanese et al., 2023), statistically significant despite the large uncertainty.

In particular, the NACFS is characterized by dextral transpression and shows the clearest evidence of recent deformation along the whole ACFS (Folguera et al., 2004). Strong Pleistocene tectonic activity in this region has been widely documented with high- and low-angle thrust faults affecting Pleistocene lavas and sediments (Folguera et al., 2004, 2006). These authors registered several cases of well-developed small-scale dextral strike-slip faults trending N to NNE. This includes the presence of sets of faults determining adjacent blocks in a domino pattern. Neotectonic deformation has also been documented by several large rockslides in the latest Pleistocene and Holocene (Penna et al., 2011). Colavitto et al. (2020) questioned the relevance of the strike-slip components in most neotectonic structures, suggesting that compression dominated the evolution of the Guañacos thrust and fold

belt in recent times. Shallow earthquake data (Milanese et al., 2023), although scarce, show dominantly N-S dextral strike-slip focal mechanisms in the study region similar to the seismic activity along the northern LOFZ. Unfortunately, no local seismic networks have been deployed in our study area to determine microseismicity.

Milanese et al. (2023) found anomalously low angular standard deviation (ASD) for virtual geomagnetic poles (VGPs) derived from reverse-polarity sites that do not replicate those of normal polarity. We note this result because Quidelleur et al. (2009) also found evidence of very low paleosecular variation in a study of Pleistocene lavas of reverse polarity (Matuyama chron) exposed some 150 km to the NE of our study zone.

With the aim of contributing to a better understanding of possible anomalous paleosecular variation in the region and whether Andean deformation involved crustal block rotations along the northern Antifuerz-Copahue fault zone (NACFZ) in the Late Pliocene and Pleistocene, additional paleomagnetic sampling was carried out on Late Pliocene volcanics exposed 16 km northwest of Andacollo (Bella Vista section; Figs. 2 and 3). We also added to this study a set of samples previously collected along the southern margin of the Huaraco River (Río Huaraco section; Fig. 3), from which only preliminary results were available (Rovere et al., 2004). This area is a transition zone between two different regional tectonic dynamics: the strike-slip LOFZ dynamics south of $\sim 38^\circ\text{S}$ and the mostly compressive tectonics of the Central Andes to the north. Although the northern limits of the LOFZ are currently under investigation, they are expected to be around this area. Our data are of interest for those regional

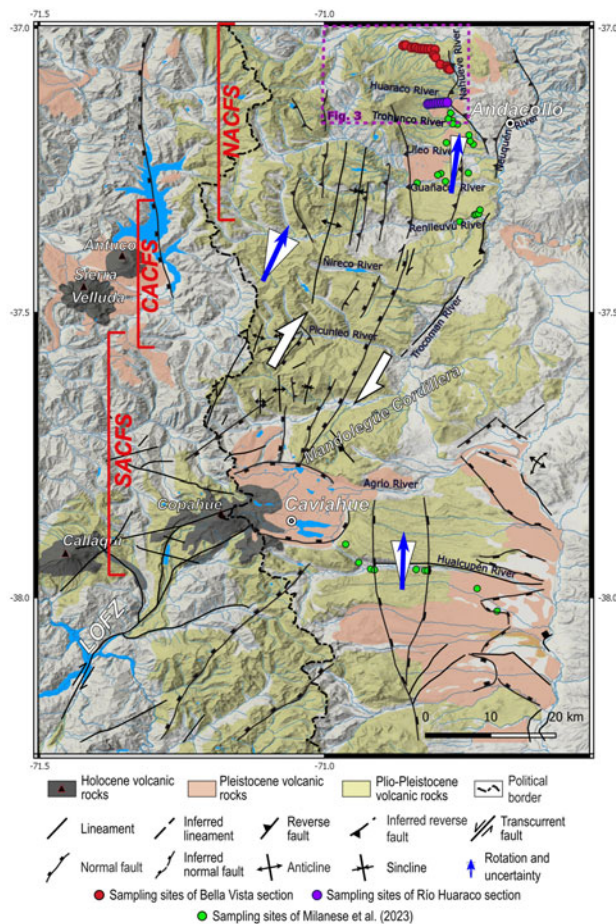


Figure 2. Plio-Holocene volcanic rocks and main structures of the Antiñir-Copahue Fault System (ACFS) area. Structures are summarized from Folguera et al. (2004), Melnick et al. (2006), and Rojas Vera et al. (2016). Paleomagnetic sampling sites correspond to this paper and to Milanese et al. (2023). Modified from Milanese et al. (2023). CACFS, central AFCS; LOFZ, Liquiñe-Ofqui Fault Zone; NACFS, northern AFCS; SACFS, southern AFCS.

tectonic studies carried out along the Central-Southern and Patagonian Andes. On the other hand, the geomagnetic implications of paleosecular variation values for this region in the Late Pliocene and Pleistocene may shed light on the evolution of the Earth's magnetic field on global and regional scales.

GEOLOGIC SETTING

The study area is in the northern Neuquén Cordillera, in the southern part of the Central Andes of Argentina. This area underwent a complex tectonic evolution in the Cenozoic, with alternating periods of crustal shortening and extension (Folguera et al., 2004, 2006, 2007, 2011; Rojas Vera et al., 2016). These have been mainly associated with changes in the subduction angle of the Nazca plate under the Andean margin (Ramos et al., 2011).

An extensional basin (between 36.50°S and 39.00°S and between 71.50°W and 70.50°W, up to 3000 m thick) developed in the study region in an intra-arc setting in the Late Oligocene–earliest Miocene (25–19 Ma; Jordan et al., 2001; Folguera et al., 2004, 2006; Rosselot et al., 2020), known as the lower section of the Cura Mallín basin (Jordan et al., 2001; Folguera et al., 2003). In the Late Miocene (16–6 Ma), an episode

of shortening led to the uplift of the Principal Cordillera at this latitude and the closure of the Cura Mallín basin (Melnick et al., 2006). This tectonic episode developed the Guañacos fold and thrust belt, which has been active since then, in the inner-axial sector of the Neuquén Cordillera. After this tectonic phase, a period of extension took place between 37.50°S and 39.00°S, opening the Cola de Zorro basin (Folguera et al., 2003) in the Plio-Pleistocene (Folguera et al., 2002).

Plio-Pleistocene volcanic rocks have a large areal distribution in the study region (Figs. 2 and 3). This work follows the criteria of Folguera et al. (2006) and Penna (2010), who incorporate this volcanism within the Cola de Zorro Formation. This unit was defined by González Ferrán and Vergara Martínez (1962) as referring to volcanic rocks of andesitic–basaltic composition with horizontal to subhorizontal attitude. Its type section is exposed in the Cola de Zorro ravine (~36.45°S, 71.09°W), north of our study area. In the retroarc, this volcanic sequence is made up of subhorizontal successions that constitute extensive plains or plateaus, formed by basalts, andesitic lavas and ignimbrites, volcanic breccias, and subordinate sedimentary rocks. The age of this sequence has been radiometrically dated between 5.7 and 1.0 Ma (López-Escobar et al., 1981; Vergara Martínez and Muñoz Bravo, 1982; Niemeyer and Muñoz, 1983; Suárez and Emparán, 1997; Linares et al., 1999; Folguera et al., 2004; Rovere et al., 2004; Burns et al., 2006).

Basalts and basaltic andesites sampled in this study are interpreted to have been erupted from the central Centinela volcano (Fig. 3) and other monogenetic cones. Rovere et al. (2004), using stratigraphic data and K-Ar radiometric dates, defined the main stage of activity of the central Centinela volcano at 2.8 ± 0.1 to 2.9 ± 0.2 Ma. They also obtained K-Ar radiometric dates corresponding to lavas coming from monogenetic cones in a time interval between 3.2 ± 0.2 and 2.6 ± 0.1 Ma. Based on this, we assigned them to the Cola de Zorro Formation, although Rovere et al. (2004) labeled Cerro Centinela Formation those lavas interpreted to come from the Centinela volcano, and Bella Vista Formation those assigned to monogenetic cones. Our choice follows the same criteria used by Milanese et al. (2023). The numerical age data obtained from nearby areas of this unit correspond to K-Ar whole-rock dates (Folguera et al., 2004) from the Guañaco (1.7 ± 0.2 Ma) and Nireco (3.1 ± 0.2 and 4.0 ± 0.5 Ma) valleys and a date of 3.8 ± 0.4 Ma ($^{40}\text{Ar}/^{39}\text{Ar}$ in hornblende; Burns et al., 2006) from the Lileo River valley (Fig. 2).

The Bella Vista section (Fig. 3) is about 136 m thick, while the Río Huaraco is about 160 m thick. Macroscopically, these rocks from the Cola de Zorro Formation generally show a porphyritic texture, with phenocrysts of plagioclase and mafic minerals in an aphanitic groundmass.

Pleistocene basaltic volcanic cones from the Guañacos Formation were formed on top of the Plio-Pleistocene plateau and are composed of olivine basalts and basaltic andesites. Rovere et al. (2004) obtained whole-rock K-Ar dates of 1.4 ± 0.2 and 1.1 ± 0.1 Ma in the Lileo-Guañaco block and of 0.9 ± 0.1 Ma in the Trohunco-Lileo block (Fig. 2). These lavas were not sampled in this study, but some of those exposures were studied by Milanese et al. (2023) and are included in the tectonic analysis.

The drainage network in the study area shows conspicuous structural and lithologic control. Main rivers run along straight valleys with an E-W orientation, probably controlled by nearly rectilinear faults (Reñileuvú, Guañaco, Lileo, etc.; Rovere et al., 2004; Folguera et al., 2006; Fig. 2). Milanese et al. (2023) speculated that these rivers define rectangular crustal blocks some

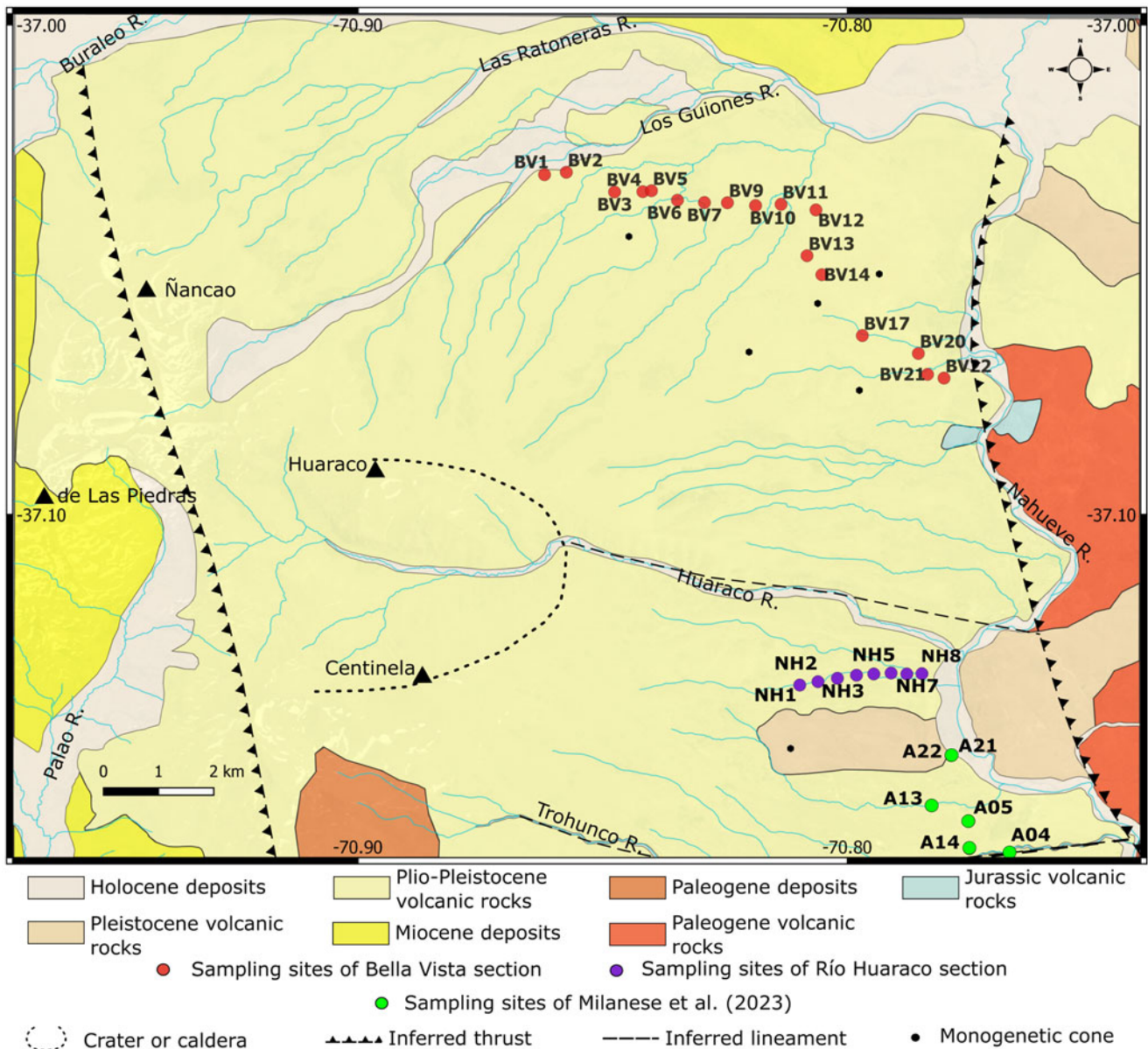


Figure 3. Geologic map of the study area (based on Rovere et al., 2004) with the location of the sampling sites. Sites BV1 to BV22 correspond to the Bella Vista section. Sites NH1 to NH8 correspond to the Río Huaraco section. Sampling sites of Milanese et al. (2023) are also shown.

5 km N-S by 10–15 km E-W that may have experienced clockwise tectonic rotation in a domino-type pattern in the last few million years. Although a mean estimate of paleomagnetic data from this area hinted at about 8° rotation, the large uncertainty in the angular parameters rendered this estimate not statistically significant.

METHODS

Oriented samples from 25 paleomagnetic sites from Bella Vista and Río Huaraco sections (Fig. 3), located in the northern areas of the ACFS (Fig. 2), were studied. All correspond to the Plio-Pleistocene volcanic rocks of the Cola de Zorro Formation, dated in the study area at 3.2 to 2.6 Ma (Rovere et al., 2004).

Samples were collected from 17 paleomagnetic sites along the Bella Vista section (Fig. 3). At each site, at least 8 cores were obtained with a gas-powered portable drill and oriented with

clinometer and magnetic and sun compasses. A total of 145 oriented samples were collected in this locality. The Río Huaraco section (Fig. 3) comprises 8 sampling sites. At each site, two or three block samples oriented with magnetic and sun compasses were collected, resulting in 21 block samples in total. At least 2 standard, 2.54-cm-diameter (1-inch-diameter) cores per block sample and at least two specimens per core were cut, providing a total of 103 oriented specimens.

Laboratory procedures and analyses were carried out at the Daniel A. Valencio Paleomagnetism Laboratory of the Instituto de Geociencias Básicas, Aplicadas y Ambientales de Buenos Aires (IGEBA). All cores were sliced into standard-size specimens (2.2 cm in height by 2.54 cm in diameter). The direction and intensity of the natural remanent magnetization were measured with a JR-6 spinner magnetometer. The usual demagnetization techniques (alternating magnetic fields and thermal approaches)

were applied to one pilot specimen per site to select the optimum experimental procedure to determine the magnetic remanence components.

Stepwise demagnetization at elevated temperatures was accomplished with an ASC TD48-SC thermal demagnetizer, in steps of 100°C, 150°C, 200°C, 250°C, 300°C, 350°C, 400°C, 450°C, 475°C, 500°C, 525°C, 550°C, 575°C, 600°C, 625°C, and 650°C. An alternating field (AF) demagnetization routine was carried out with an ASC D-2000 tumbler demagnetizer in steps of 3, 6, 9, 12, 15, 20, 25, 30, 35, 40, 50, 60, 75, 90, 105, 120, 140, and 160 mT. After analysis of the results of the pilot procedures, AF demagnetization was considered the most effective and was applied to the rest of the samples. Results from a previous pilot study on 37 specimens from the Río Huaraco section were added to our results. In that pilot study, one specimen from each site was subjected to AF demagnetization up to 20 mT followed by thermal demagnetization (11 increasing stages from 100°C to 580–650°C) and two or three specimens were subjected to an initial thermal demagnetization at 150°C followed by AF demagnetization (13 stages from 3 to 110 mT). In that case, remanence measurements were carried out with a 2G–550R cryogenic magnetometer, AF demagnetization with a static three axes degausser attached to the magnetometer, and high-temperature demagnetization with a Schonstedt TS-1 demagnetizer.

Each specimen's behavior was analyzed using the Remasoft (AGICO) program. Components were defined by principal component analysis (PCA; Kirschvink, 1980).

Rotations along vertical axes (R), inclination anomalies (IA), and their uncertainties were calculated following Demarest (1983) and Beck (1989).

The bulk susceptibility (k_m) of the specimens was measured with a Kappabridge MKF1-A (AGICO) susceptibilimeter. The same instrument was used to measure k as a function of the intensity of the applied magnetic field, for a representative specimen per site. Plots of bulk susceptibility as a function of field intensity (5 to 700 A/m) at a fixed frequency (f_1) of 976 Hz were obtained. In addition, susceptibility measurements at 200 A/m with two different frequencies, f_1 (976 Hz) and f_3 (15,616 Hz), were obtained from the same specimens.

The variations of the magnetic susceptibility with respect to the intensity and frequency of the applied magnetic field were studied to help in the identification of the ferrimagnetic (s.l., *sensu lato*) minerals carried by the rocks and their domain state, respectively.

Five specimens were selected, three from the Bella Vista section and two from the Río Huaraco section, to perform magnetization and remanence hysteresis cycles with a vibrating sample magnetometer (Molspin) as well as high-temperature thermomagnetic curves (k vs. T) with a MFK.1A susceptibilimeter and a CS-3 device in an Ar-rich atmosphere.

RESULTS

Magnetic properties

The bulk magnetic susceptibility of the Bella Vista cross-section ranges from 9.48 to 42.11×10^{-3} SI (International System of Units), while the Río Huaraco section shows values between 1.30 and 37.10×10^{-3} SI.

Normalized bulk susceptibility variation (K/K_{\min}) versus intensity of applied field for samples from all sites is shown in Figure 4. Two groups are distinguished. Sites BV3, BV7, BV11,

BV13, BV20, NH1, NH5, and NH6 do not show significant variations in susceptibility with the applied field. The other group presents an increase in susceptibility with the applied field. A subgroup (BV2, BV9, BV22, and NH8) increases its susceptibility significantly more than the other and most numerous subgroup (BV1, BV4, BV5, BV6, BV10, BV12, BV14, BV17, BV21, NH2, NH3, NH4, and NH7) with relatively minor increases of 1–6%.

Field intensity dependence of the magnetic susceptibility was quantified by Eq. 1:

$$K_{HD}(\%) = 100 * \frac{(k_{200} - k_{20})}{k_{200}} \quad (Eq.1)$$

where k_x is the susceptibility measured in the respective amplitude field, expressed in A/m (Chadima et al., 2009).

K_{HD} values range from 0% to 4.8% (Table 1). This means that the increase in susceptibility with the magnetic field from 20 A/m to 200 A/m does not exceed 5%. Therefore, the magnetic susceptibility of these samples is likely dominated by (Ti-poor) magnetite.

It can be inferred from Figure 4 that magnetite is the likely magnetic carrier in the group that does not show significant variations in susceptibility with the applied field (sites BV3, BV7, BV11, BV13, BV20, NH1, NH5, and NH6). The remaining samples are probably dominated by Ti-poor titanomagnetite, with higher Ti content in those samples with a greater increase in susceptibility (Chadima et al., 2009).

The frequency dependence of magnetic susceptibility is characterized as:

$$K_{FD}(\%) = 100 * \frac{(k_{F1} - k_{F3})}{k_{F1}} \quad (Eq.2)$$

where k_{F1} and k_{F3} are susceptibilities at frequencies F_1 (976 Hz) and F_3 (15,616 Hz), measured in a field of 200 A/m (Dearing et al., 1996).

As Hrouda (2011) proposes, the K_{FD} parameter was normalized, obtaining the K_{FB} :

$$K_{FB}(\%) = \frac{\ln 10}{\ln f_{mF3} - \ln f_{mF1}} * K_{FD} \quad (Eq.3)$$

where f_m is the operating frequency.

Regarding the dependence of susceptibility with frequency, the K_{FD} parameter was used, obtaining values between 2.5% and 3.6% for the Bella Vista section and between 1.2% and 10.2% for the Río Huaraco section (Table 2). This means a very weak dependence of k with frequency, except for the NH5 site. This suggests an insignificant contribution of superparamagnetic grains, except at the NH5 site, where a large percentage of small particles can be inferred. Furthermore, this is the site with the lowest susceptibility, on the order of 1×10^{-3} SI.

Thermomagnetic curves (Fig. 5) show irreversible behavior, due to the formation of new minerals from heating. Heating curves show main magnetic phase with Curie temperatures between 580°C and 600°C, with the exception of site NH5, whose Curie temperature is about 640°C. Therefore, magnetite is the principal magnetic phase, with possible subsidiary contribution of hematite or maghemite.

Samples from Bella Vista (sites BV1, BV7, and BV14) and Río Huaraco (sites NH4 and NH5) present similar hysteresis curves (Fig. 6). These samples exhibit strong ferrimagnetic behavior

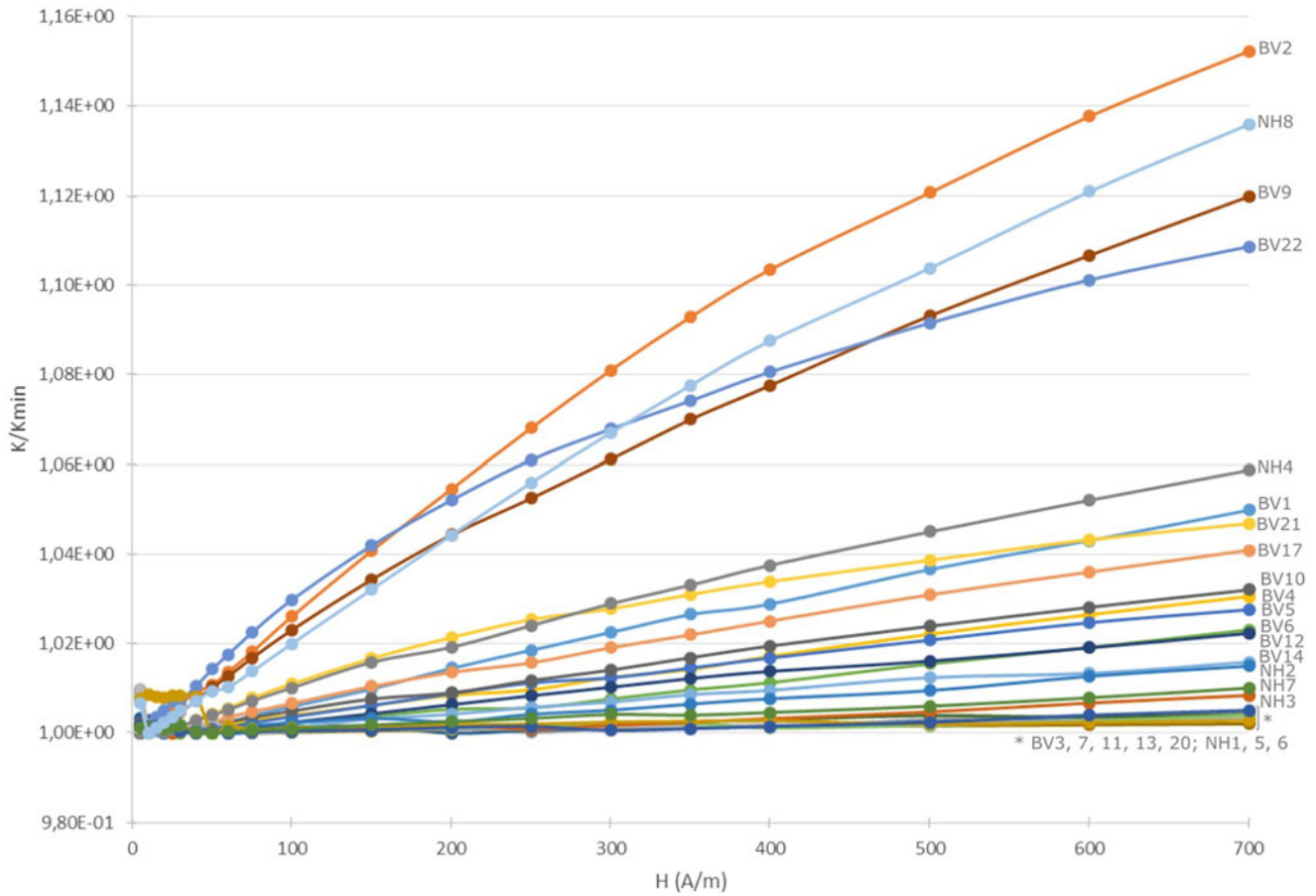


Figure 4. Bulk magnetic susceptibility as a function of the intensity of the applied magnetic field, from 5 to 700 A/m, at a frequency of 976 Hz.

Table 1. Dependence of bulk susceptibility on the applied magnetic field quantified by means of K_{HD} , for each site

Site	K_{HD} (%)	Site	K_{HD} (%)	Site	K_{HD} (%)	Site	K_{HD} (%)	Site	K_{HD} (%)
BV1	1.37	BV6	0.413	BV12	0.543	BV21	1.92	NH4	1.87
BV2	4.79	BV7	-0.0823	BV13	-0.0284	BV22	4.47	NH5	-0.601
BV3	-0.048	BV9	3.93	BV14	0.389	NH1	0.00489	NH6	-0.00502
BV4	0.659	BV10	0.892	BV17	1.22	NH2	0.255	NH7	0.151
BV5	0.798	BV11	-0.0382	BV20	-0.0385	NH3	0.0536	NH8	4.01

Table 2. Values of percentage of K_{FD} and K_{FB} frequency dependence, for each site

Site	K_{FD} (%)	K_{FB} (%)	Site	K_{FD} (%)	K_{FB} (%)	Site	K_{FD} (%)	K_{FB} (%)	Site	K_{FD} (%)	K_{FB} (%)
BV1	2.90	2.40	BV9	3.44	2.86	BV20	3.56	2.96	NH5	10.20	8.47
BV2	3.45	2.87	BV10	3.23	2.68	BV21	3.10	2.57	NH6	1.73	1.44
BV3	2.91	2.42	BV11	3.03	2.52	BV22	3.13	2.60	NH7	1.67	1.39
BV4	2.97	2.47	BV12	3.36	2.79	NH1	1.53	1.27	NH8	1.98	1.64
BV5	2.89	2.40	BV13	3.20	2.66	NH2	1.25	1.04			
BV6	2.97	2.47	BV14	3.53	2.93	NH3	2.05	1.70			
BV7	2.51	2.08	BV17	3.09	2.57	NH4	1.50	1.25			

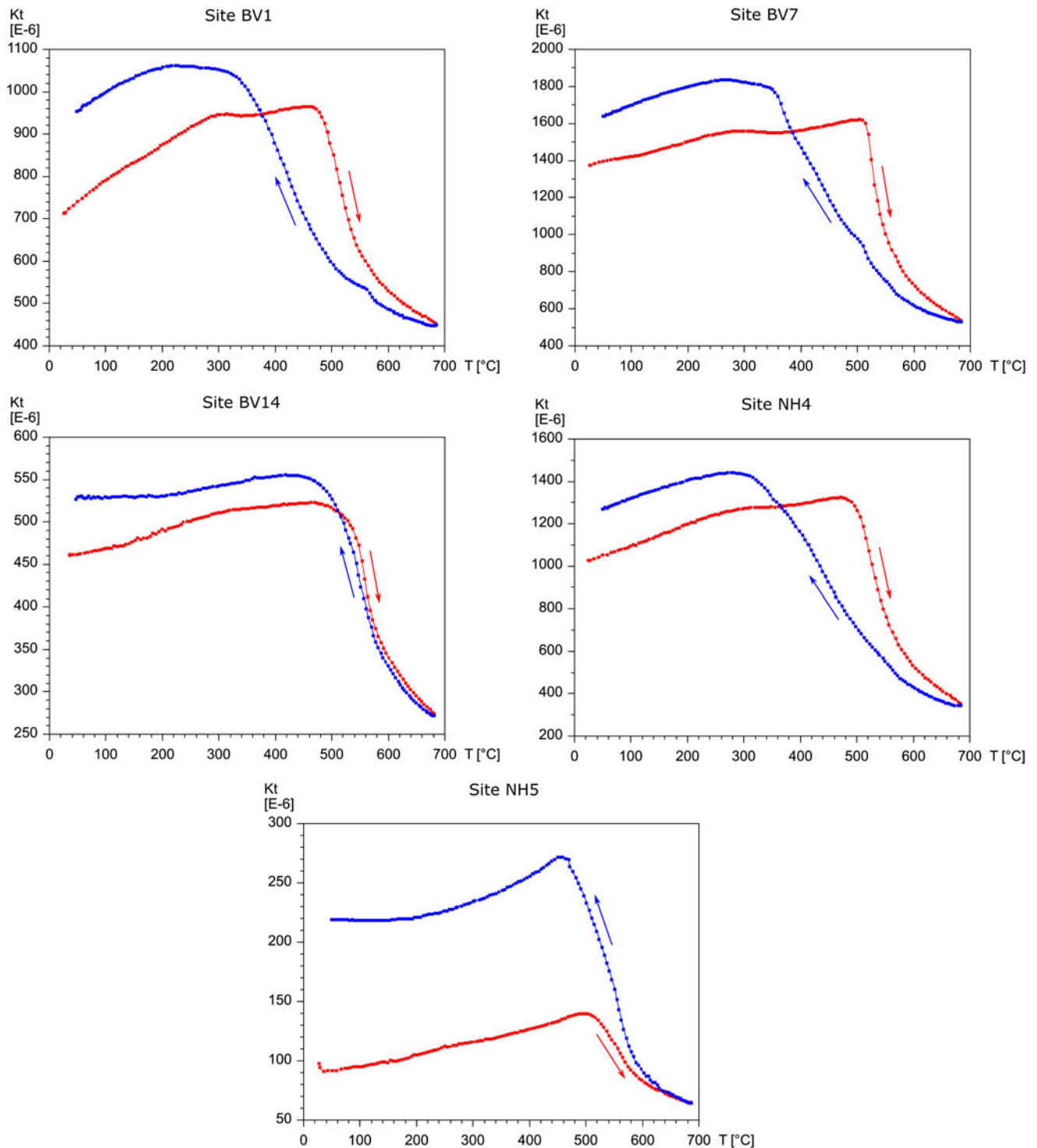


Figure 5. Thermomagnetic curves of samples from Bella Vista (sites BV1, BV7, and BV14) and Río Huaraco (sites NH4 and NH5) sections.

with low coercive force values (H_C between 3.6 and 9.6 mT), except for the NH5 site, where the coercive force is higher (H_C : 28.9 mT) and shows a larger paramagnetic influence. In addition, NH5 has a wasp waist, probably due to the presence of superparamagnetic minerals or to the mixture of one phase with high coercivity (hematite?) and the other with low coercivity (magnetite?). Hematite is a likely product of deuteritic alteration.

On the other hand, all samples reach saturation by 600 mT, with saturation magnetization values (M_s) between 0.13 and 1.77 Am^2/kg . This indicates that ferrimagnetic phases dominate all hysteresis loops. Paramagnetic as well as occasional anti-ferromagnetic contributions look subordinate.

Isothermal remanence acquisition curves show the dominance of ferrimagnetic (*sensu lato*) minerals, with remanence coercive

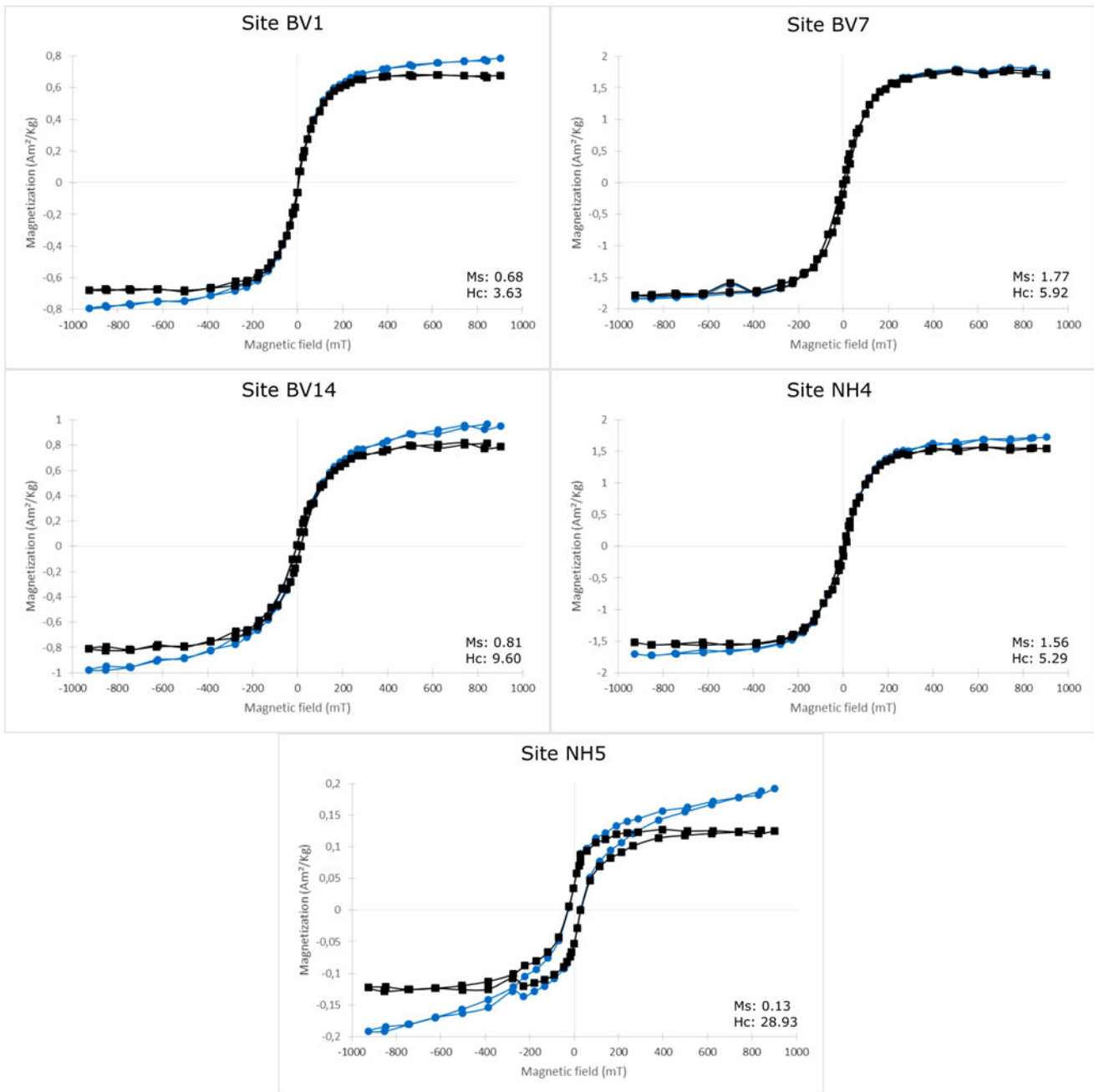


Figure 6. Hysteresis cycles of samples from Bella Vista (sites BV1, BV7, and BV14) and Río Huaraco (sites NH4 and NH5) sections, after subtracting the paramagnetic component (black curve) and before performing the subtraction (blue curve). Hc is the coercive field in mT and Ms is the saturation magnetization in Am²/kg.

force values (Hcr) between 21.6 and 59.9 mT (Fig. 7). Specimens reach saturation at fields around 600 to 700 mT. Site NH5 sample does not reach saturation and is the one with the greatest coercive force, which confirms contribution of both magnetite and hematite.

Demagnetization results

A total of 247 demagnetized specimens yield characteristic remanent magnetization (ChRMs) that can be interpreted and computed by PCA (Kirschvink, 1980); 144 specimens correspond to Bella Vista and 103 to Río Huaraco. There is no significant difference between directions of the ChRMs obtained by thermal

demagnetization versus those from AF demagnetization at any site from the Bella Vista section (Fig. 8). However, samples from the Río Huaraco site do not respond well to thermal demagnetization.

Because most specimens of the Bella Vista section are completely unblocked at temperatures near 575°C (Fig. 8), the most likely carrier of the magnetization is (Ti-poor) magnetite, as strongly suggested by the rock magnetic studies. Two components were observed, with the presence of hematite in only in a few samples, such as that of BV1 site (BV1-9.2; Fig. 8), with the highest laboratory unblocking temperature found on samples at this site about 650°C. For the Río Huaraco section, hematite is more frequent, as shown by full unblocking at temperatures

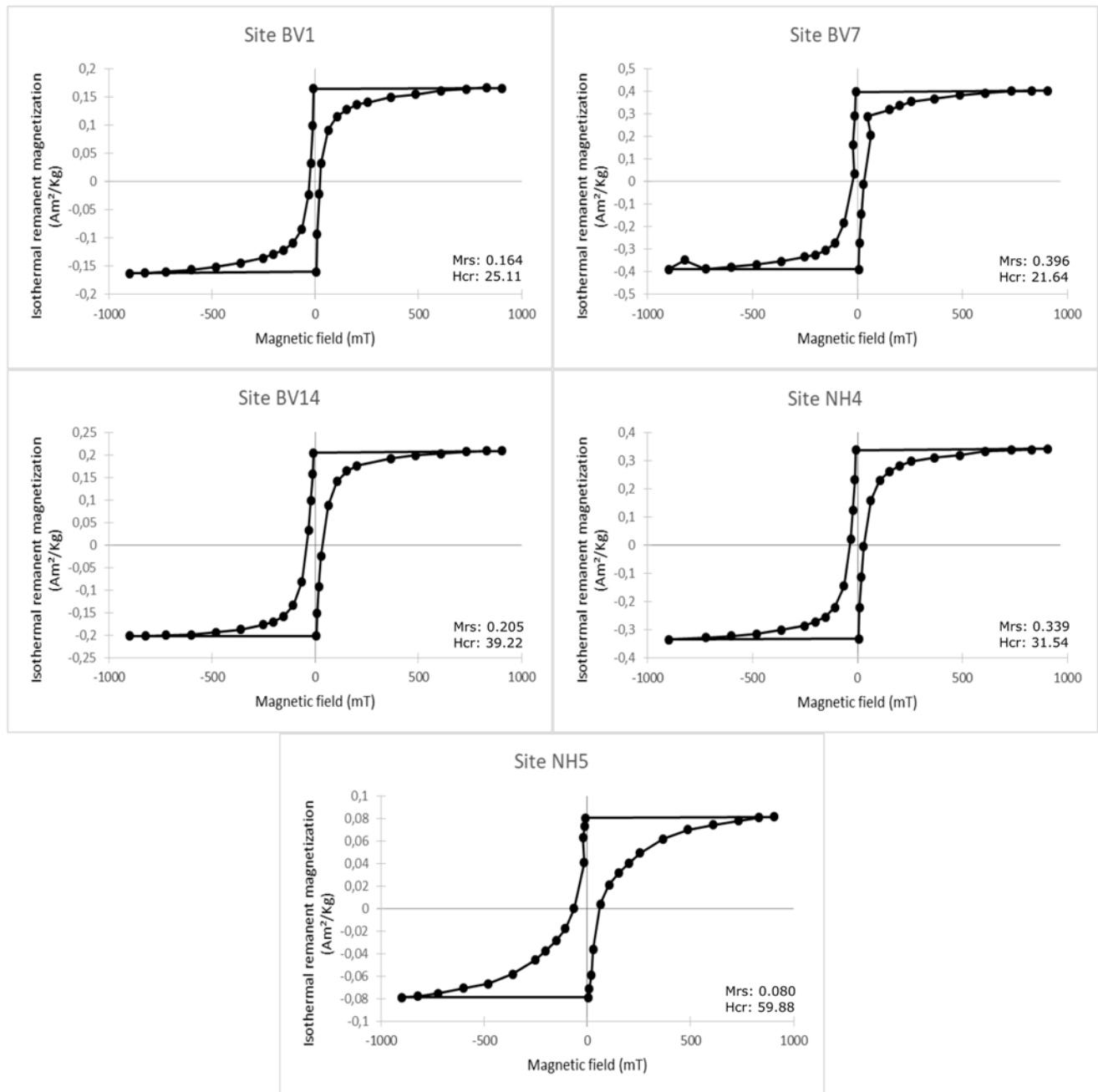


Figure 7. Isothermal remanence acquisition curves of samples from Bella Vista (sites BV1, BV7, and Bv14) and Río Huaraco (sites NH4 and NH5) sections.

close to 650°C (Fig. 8) and to a lesser extent at 575°C. Therefore, the likely carriers of magnetization at this section are interpreted to be both hematite and magnetite. A thermoremanent magnetization was likely acquired by magnetite during cooling, while hematite could have formed at early stages during deuteric alteration (e.g., Geissman and Van der Voo, 1980).

Paleomagnetic directional analysis

Bella Vista

Estimated mean directions were determined for ChRMs at each site. Of the 17 sampling sites (Fig. 9), two were rejected due to their high within-site dispersion (sites BV4 and BV12). The other sites

have within-site directional consistency, with $\alpha_{95} < 10^\circ$, and in most cases $\alpha_{95} < 5^\circ$ (Table 3).

All sites have estimated mean directions of negative inclination indicating the recording of a geomagnetic field of normal polarity. No bedding correction was applied to the characteristic directions, because the flows were determined as horizontal in the field.

VGPs were calculated from the estimated site mean directions (Fig. 9, Table 3). The BV21 and BV22 site directions are anomalous (Fig. 9), suggesting that they record a transitional magnetic field. These sites were also excluded from estimating the grand mean of the Bella Vista section.

Directions from sites BV2 and BV3, as well as BV6 and BV7, are grouped into single estimated mean directions, as they cannot

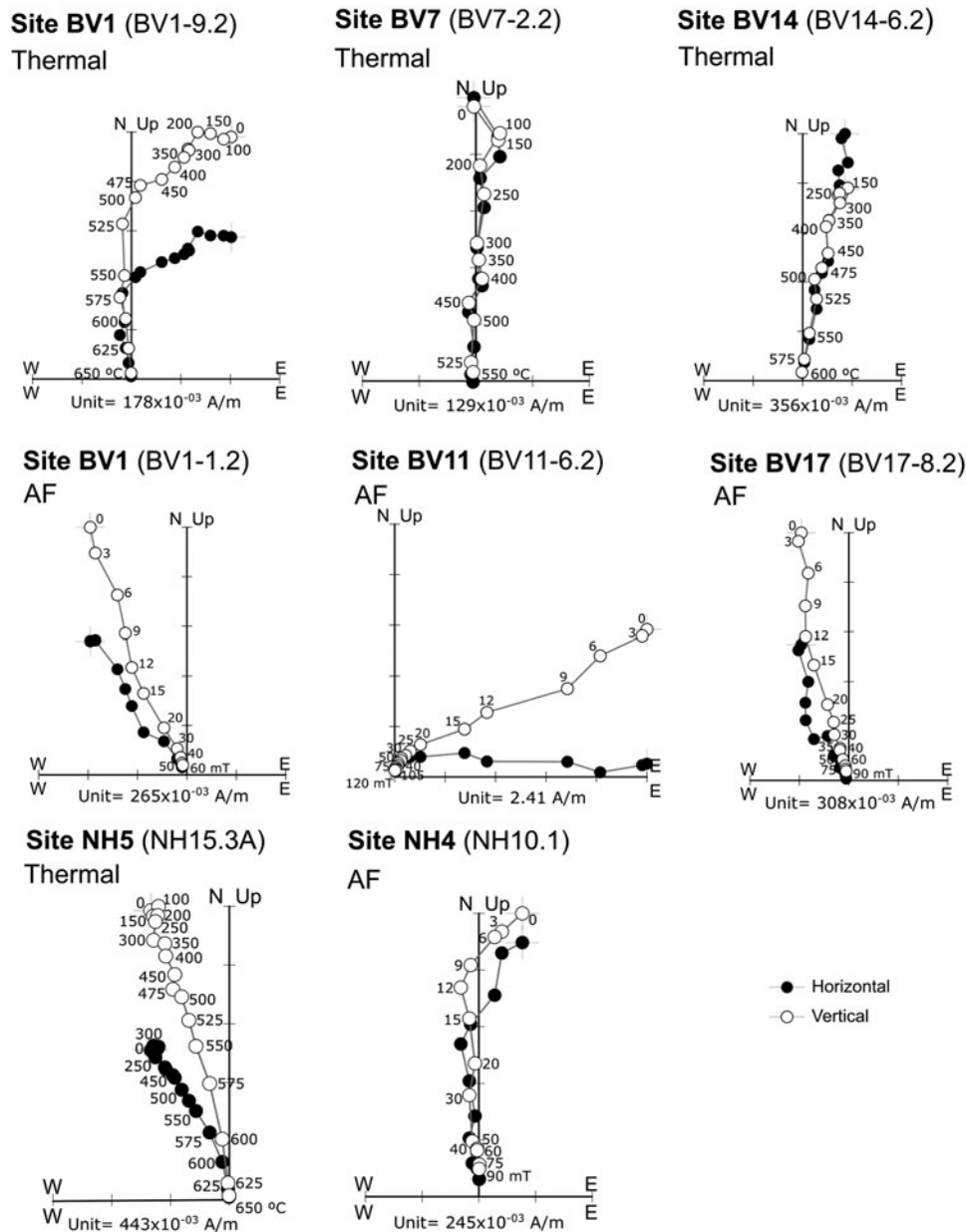


Figure 8. Orthogonal demagnetization diagrams (Zijderveld, 1967) for six samples of the Bella Vista section and two samples of the Río Huaraco profile. The specimens from BV1, BV7, BV14, and NH5 sites were demagnetized by thermal methods and those from BV1, BV11, BV17, and NH4 sites by AF methods.

be statistically distinguished from each other and are interpreted as representing the same cooling units (Fig. 9).

From the 11 VGPs computed from the independent lavas sampled along this section (Table 3), the calculated pole is located at 289.3°E and 83.7°N ($K = 28.8$ and $A_{95} = 8.7^\circ$).

Río Huaraco

The eight sites yield good within-site directional consistency, with $\alpha_{95} < 10^\circ$ (Table 4). As in the Bella Vista case, all sites show mean ChRM directions of negative inclination corresponding to a normal polarity field (Fig. 9). No bedding correction was applied, as the flows are horizontal.

Mean directions per site and the corresponding VGPs are shown in Table 4 and Figure 9. From the eight VGPs, a mean

VGP located at 189.1°E and 85.9°N ($K = 55.7$ and $A_{95} = 7.5^\circ$) is obtained.

The estimated mean site ChRM directions for the Bella Vista and Río Huaraco sections (Fig. 10) are roughly consistent with the expected mean direction for the locality from the <5 Ma global paleomagnetic pole obtained by Torsvik et al. (2012), located at 88.5°N and 353.9°E, corresponding to Dec = 358.3°, Inc = -57.1°, and $\alpha_{95} = 1.9^\circ$. Mean estimated directions from each section cannot be statistically distinguished according to the *F*-test of Watson (1956) with a 95% confidence (Fig. 10).

For both sections, an overall estimated mean direction with $N = 19$, Dec = 358.0°, Inc = -53.0°, $R = 18.6$, $K = 41.0$, and $\alpha_{95} = 5.3^\circ$ was calculated. The 19 VGPs (Tables 3 and 4) yield a mean paleomagnetic pole located at 263.8°E and 86.2°S ($K = 30.1$ and $A_{95} = 6.2^\circ$).

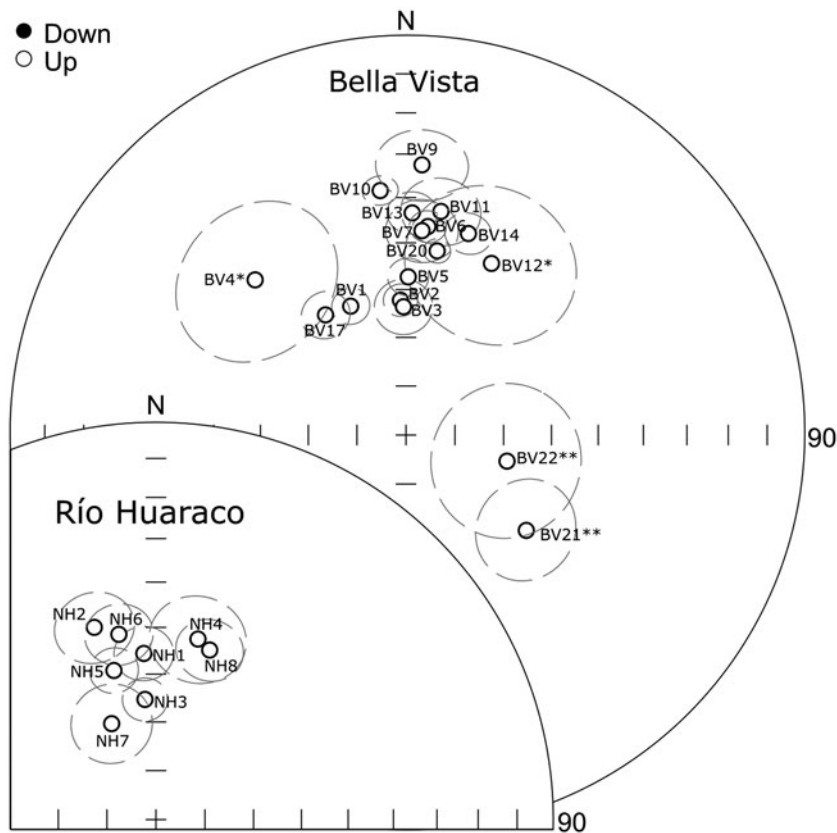


Figure 9. Equal area projection of estimated mean directions of the sites from the Bella Vista (BV) and Río Huaraco (NH) sections and their corresponding projected α_{95} values. *Sites rejected due to high intra-site dispersion. **Sites excluded for presenting anomalous directions.

DISCUSSION

Age of the studied flow sequences

Although ages of the Cola de Zorro Formation span from 5.7 ± 0.1 Ma (Linares et al., 1999) to 1.0 ± 0.1 Ma (López-Escobar et al., 1981), these values came from sites distributed over a vast area of the Andes, from $\sim 35^{\circ}\text{S}$ to 40°S . As mentioned in “Geologic Setting,” numerical ages of the studied lavas in the Nahueve-Huaraco-Trohunco block (Fig. 3) range between 3.2 and 2.6 Ma (Rovere et al., 2004). The exclusive normal polarity yielded by all studied sites is consistent with the recording of the field during the Gauss normal polarity chron (3.596–2.595 Ma; Gradstein et al., 2020).

Geomagnetic implications

The Río Huaraco section has a mean inclination consistent with that corresponding to the global reference paleomagnetic pole of Torsvik et al. (2012) and the modern geocentric axial dipole (GAD) direction (Table 4). The inclination anomaly is virtually null ($IA = 0.1^{\circ} \pm 6.2^{\circ}$ with respect to the former, and $-0.5^{\circ} \pm 6.0^{\circ}$ with respect to the latter). Positive (negative) IA values imply lower (higher) inclinations than the reference. However, the Bella Vista section mean direction has a slightly significant shallower inclination value than expected, based on the same reference pole ($IA = 7.1^{\circ} \pm 6.2^{\circ}$) and the modern GAD ($6.4^{\circ} \pm 6.1^{\circ}$; Table 3). Averaging results from both sections yields no significant inclination anomaly with respect to the reference direction ($IA = 4.1^{\circ} \pm 4.5^{\circ}$) and the GAD ($IA = 3.5^{\circ} \pm 4.2^{\circ}$), suggesting adequate average of paleosecular variation (Table 5). The reason for a

greater IA in Bella Vista than in Río Huaraco could be due to a very minor undetected tilting of the lavas. As discussed later, an incomplete paleosecular average does not seem to be an adequate explanation. Milanese et al. (2023) also determined no significant IA in the mean direction from 17 Late Pliocene and Pleistocene lavas of both polarities exposed immediately to the south of our study localities (Fig. 11). Similar results were obtained by Quidelleur et al. (2009) on Early Pleistocene lavas of reverse polarity and on <300 ka lavas of normal polarity, around 150 to 250 km to the NE of our sites (Fig. 11). Moncinhatto et al. (2023) carried out a paleomagnetic study about 80 to 100 km south of our study area (Fig. 11) on Early Pliocene to Late Pleistocene lavas, with most of their results corresponding to Gauss and Brunhes chrons. They found no IA when computing the mean direction from all sites with $k > 100$. A separate analysis of the Late Pliocene (Gauss chron) and the Middle to Late Pleistocene (Brunhes chron) data set shows virtually identical mean directions from lavas from both chrons (see Table 5) and a very minor to insignificant IA.

Angular dispersion values estimated from Bella Vista and Río Huaraco sections VGPs were compared with a global data set for 0–5 Ma (compiled by Moncinhatto et al., 2023) and with the models proposed by McFadden et al. (1988), Bono et al. (2020), Brandt et al. (2020), and de Oliveira et al. (2021; Fig. 11). When comparing the ASD of the VGPs calculated for each section with the global database for 37°S , ASDs for the Bella Vista (15.2°) and the Río Huaraco (14.2°) sections are consistent with expected values. Considering both sections together, the angular dispersion ($ASD = 14.8^{\circ}$) also is close to the expected values from all recent geomagnetic models (Fig. 11). As discussed by

Table 3. Characteristic remanent magnetization estimated mean directions per site for the Bella Vista section

<i>Mean direction</i>							<i>Sampling site</i>		<i>VGP^a</i>	
Site	n/n ₀	Dec (°)	Inc (°)	R	k	α ₉₅ (°)	Lat. (°)	Long. (°)	Pole lat. (°)	Pole long. (°)
BV1	10/10	336.8	-61.1	9.94	160.4	3.8	-37.031	-70.862	71.5	175.9
BV2	8/8	357.7	-62.2	7.97	265.1	3.4	-37.030	-70.857	—	—
BV3	8/8	358.9	-63.6	7.92	92.2	5.8	-37.034	-70.848	—	—
BV2&3	16/16	358.3	-62.9	15.90	144.5	3.1	-37.030	-70.850	82.6	118.7
BV4 ^b	8/8	315.8	-44.7	7.43	12.3	16.4	-37.034	-70.842	—	—
BV5	8/8	0.8	-57.3	7.96	190.5	4.0	-37.034	-70.840	88.9	72.2
BV6	8/8	6.0	-46.2	7.97	251.8	3.5	-37.036	-70.835	—	—
BV7	8/8	4.5	-47.2	7.89	65.7	6.9	-37.036	-70.829	—	—
BV6&7	16/16	5.2	-46.7	15.86	110.6	3.5	-37.036	-70.830	79.9	-43.5
BV9	8/9	3.4	-32.4	7.85	45.9	8.3	-37.036	-70.825	70.3	-61.0
BV10	8/8	354.0	-38.1	7.97	276.9	3.3	-37.037	-70.819	73.6	-90.8
BV11	8/8	8.9	-42.5	7.87	55.2	7.5	-37.037	-70.814	75.4	-36.7
BV12 ^b	5/8	26.5	-50.1	4.81	21.5	16.9	-37.038	-70.806	—	—
BV13	9/10	1.6	-43.4	8.93	119.3	4.7	-37.047	-70.808	78.2	-63.9
BV14	8/8	17.2	-45.9	7.95	152.9	4.5	-37.051	-70.805	72.6	-9.8
BV17	9/9	326.2	-60.2	8.93	111.1	4.9	-37.063	-70.797	63.6	179.7
BV20	6/8	9.6	-51.2	5.99	663.2	2.6	-37.067	-70.786	80.5	-11.2
BV21 ^c	9/9	128.4	-58.3	8.69	26.1	10.3	-37.071	-70.784	—	—
BV22 ^c	8/10	104.5	-68.6	7.48	13.5	15.6	-37.072	-70.780	—	—
<i>Mean paleomagnetic direction</i>										
Section	N	Dec (°)	Inc (°)	R	K	α ₉₅ (°)				
Bella Vista	11	0.0	-50.0	10.7	36.8	7.6				
<i>Reference mean direction from Torsvik et al. (2012)</i>										
Dec (°)	Inc (°)	α ₉₅ (°)	Age (Ma)							
358.3	-57.1	1.9	<5							
<i>Modern axial geocentric dipole direction</i>										
Dec (°)	Inc (°)									
0.0	-56.4									

^aVirtual geomagnetic poles (VGPs) calculated for each site of the Bella Vista section.

^bSite excluded due to high intra-site dispersion.

^cSite excluded for having anomalous directions.

Moncinhatto et al. (2023), our data support the hypothesis that the GAD can account for most of the paleodirections reported in this area of South America for the period studied and that if a contribution from non-dipole components is required to model time-averaged field determinations, this should be rather small.

These data are comparable to those obtained by Quidelleur et al. (2009), at ~36°S (see Table 5), who reported an ASD = 14.8° for Pleistocene lavas of both polarities in the Payún Matrú and Cerro Nevado volcanic massifs. However, their study reported an ASD = 16.5° for normal polarity (Brunhes chron) VGPs and an ASD = 12.5° for reverse-polarity data (Matuyama chron;

Table 5). The latter value is lower than those predicted by traditional and recent paleosecular variation models for these latitudes. Low paleosecular variation during the Matuyama reverse chron found by Quidelleur et al. (2009) for this region was recently confirmed by Milanese et al. (2023) in their study of lavas of Cola de Zorro and Guañacos Formations, a few tens of kilometers south of our study locality (Fig. 11). They found ASD = 14.7° for the normal polarity VGPs and ASD = 11.7° for the reverse population.

Table 5 summarizes that in the southern Central Andes region of Argentina, VGPs of the normal polarity Gauss (Late Pliocene) and Brunhes (Middle and Late Pleistocene) chrons show expected ASD, while reverse-polarity Matuyama (Early Pleistocene) chron

Table 4. Mean direction per site for the ChRM component of the Río Huaraco section and virtual geomagnetic poles (VGPs) for each site at Río Huaraco

Mean direction							Sampling site		VGP	
Site	n/n ₀	Dec (°)	Inc (°)	R	k	α ₉₅ (°)	Lat. (°)	Long. (°)	Pole lat. (°)	Pole long. (°)
NH1	14/16	355.8	-55.5	13.73	47.7	5.8	-37.13	-70.80	86.5	-145.8
NH2	15/15	342.2	-47.9	14.46	25.9	7.7	-37.13	-70.80	73.0	-137.5
NH3	17/17	354.8	-65.2	16.75	65.0	4.5	-37.13	-70.80	79.1	128.3
NH4	10/11	13.1	-51.5	9.67	27.1	9.4	-37.13	-70.80	78.2	-1.2
NH5	13/14	344.3	-58.0	12.84	77.0	4.8	-37.13	-70.79	77.5	-173.1
NH6	8/8	348.7	-50.7	7.90	70.7	6.6	-37.13	-70.79	79.1	-133.2
NH7	9/9	335.2	-68.3	8.80	40.8	8.2	-37.13	-70.79	67.3	151.9
NH8	13/13	17.6	-53.1	12.70	40.5	6.6	-37.13	-70.79	75.3	11.0

Mean paleomagnetic direction						
Section	N	Dec (°)	Inc (°)	R	K	α ₉₅ (°)
Río Huaraco	8	354.9	-57.0	7.9	55.7	7.5

Reference mean direction from Torsvik et al. (2012)			
Dec (°)	Inc (°)	α ₉₅ (°)	Age (Ma)
358.3	-57.1	1.9	<5

Modern axial geocentric dipole direction		
Dec (°)	Inc (°)	
0.0	-56	

VGPs show anomalously low ASD, suggesting low paleosecular variation. This enigmatic behavior of the regional magnetic field in the Early Pleistocene needs further investigation.

Tectonic implications

From comparison between mean direction of ChRM and reference direction for 0–5 Ma (Torsvik et al., 2012) for the Bella

Vista section ($R = 1.7^\circ \pm 9.7^\circ$, $IA = 7.1^\circ \pm 6.2^\circ$) and for Río Huaraco ($R = -3.4^\circ \pm 11.3^\circ$, $IA = 0.1^\circ \pm 6.2^\circ$), no significant tectonic rotation around a vertical axis occurred in the study area, since around 2.6 Ma. Merging results from both sections show very similar results ($R = -0.3^\circ \pm 7.3^\circ$ and $IA = 4.1^\circ \pm 4.5^\circ$).

Milanese et al. (2023) sites were distributed from near the Trohuncu River, less than 2 kms to the south of the Río Huaraco section, to the Reñileuvú River, over 20 km to the south (Fig. 2).

Sites at the Bella Vista locality are situated north of the Río Huaraco and the northern boundary proposed by Milanese et al. (2023) for the northernmost block potentially affected by a clockwise tectonic rotation. On the other hand, sites belonging to the Río Huaraco section correspond to the northernmost of Milanese et al. (2023) hypothetical blocks (the so-called Huaraco-Trohuncu block; Fig. 10). In fact, the northernmost sites reported by Milanese et al. (2023; i.e., A5, A13, A21, and A22) are in the same block as those from our Río Huaraco section (Fig. 3). Combining them with those from the Río Huaraco section yields an estimated locality mean for the Huaraco-Trohuncu block of $Dec = 355.7^\circ$, $Inc = -57.0^\circ$, $N = 12$ sites, $K = 70.0$, $\alpha_{95} = 5.2^\circ$. Compared with the expected direction from the 0–5 Ma reference paleomagnetic pole ($Dec = 358.3^\circ$, $Inc = -57.2^\circ$, $A_{95} = 1.9^\circ$; Torsvik et al., 2012), the mean direction for the block shows insignificant rotation ($-2.6^\circ \pm 7.9^\circ$; Fig. 12) with an irrelevant $IA = 0.2^\circ \pm 4.4^\circ$.

The remaining sites from Milanese et al. (2023) correspond to other three blocks located to the south (Fig. 12). The number of sites in each individual block is not enough to compute useful individual mean directions to evaluate small tectonic rotations,

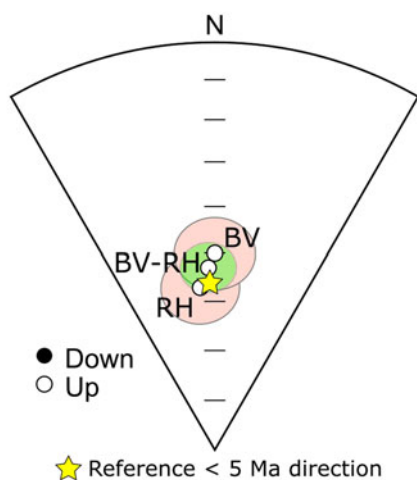


Figure 10. Grand mean estimated directions from the Bella Vista (BV) and the Río Huaraco (RH) sections. The star represents the reference direction calculated from the reference South America pole for <5Ma (Torsvik et al., 2012).

Table 5. Mean paleomagnetic data from Plio-Pleistocene volcanics in the southern Central Andes region of Argentina

Locality	Geologic unit	Age (Ma)	Polarity	Chron	Dec (°)	Inc (°)	α_{95} (°) (N)	IA (°)	ASD (°)
Caviahué-Copahué ^a	Cola de Zorro, Las Mellizas, Copahué	5.6–0.0	N (R)	Gilbert-Gauss-Brunhes	356.2	–51.5	3.9 (42)	5.8 ± 3.1	15.3
	Las Mellizas	2.68–2.60	N	Gauss	356.0	–50.3	5.0 (20)	7.0 ± 4.0	14.4
	Copahué	1.0–0.0	N	Brunhes	357.5	–49.0	8.1 (14)	8.3 ± 6.5	16.7
Bella Vista and Río Huaraco sections ^b	Cola de Zorro	3.2–2.6	N	Gauss	358.0	–53.0	5.3 (19)	3.5 ± 4.2	14.8
Trohunco-Lileo-Guañaco-Reñileuvú ^c	Cola de Zorro, Guañacos	3.8–0.9	R-N	Matuyama (Gauss)	6.4	–57.5	5.6 (17)	–1.0 ± 4.5	14.9
		3.8–2.6	N	Gauss	358.6	–53.3	9.6 (8)	3.3 ± 7.7	14.7
		2.6–0.9	R	Matuyama	194.8	60.7	5.6 (9)	–4.1 ± 4.5	11.7
Payún Matru – Cerro Nevado ^d	Llancanelo and Payún Matru volcanic fields	1.9–0.9	N	Brunhes	354.8	–53.0	6.8 (19)	2.5 ± 5.4	16.5
			R	Matuyama	181.0	52.3	5.9 (12)	3.2 ± 4.7	12.5

^aMoncinhatto et al. (2023).^bThis study.^cMilanese et al. (2023).^dGuidelleur et al. (2009).

as already acknowledged by these authors. Considering the three blocks together, 12 independent mean paleomagnetic directions are available, from both Guañacos and Cola de Zorro Formations. Nine correspond to a reverse-polarity field (five from Guañacos Formation and four from Cola de Zorro Formation) and only three to normal polarity (two from Cola de Zorro and one from Guañacos). The grand mean of those 12 site directions is Dec = 192.7°, Inc = 56.7° (N = 12, K = 41.0, α_{95} = 6.9°). Computation of R and IA values yields a statistically significant clockwise rotation of R = 14.4° ± 10.3° (Fig. 12) and IA = –0.5° ± 5.7°.

The roughly E-W, nearly rectilinear, Huaraco, Trohunco, Lileo, Guañaco, and Reñileuvú Rivers are undoubtedly structurally controlled (e.g., Rovere et al., 2004). Their narrow valleys show abrupt negative relative topographic reliefs of 100 to 200 m with respect to the plateau-like surface of the blocks they limit. They also function as boundaries for several of the Andean faults that constitute the NACFS, as well as producing changes in the dip angles and/or horizontal displacements of some of the major faults that cut across them (Folguera et al., 2004). They also seem to work as limits for outcrops of Plio-Pleistocene units that do not continue from one block into the next (Fig. 2). Milanese et al. (2023) were the first to propose that these parallel faults define a series of nearly rectangular, around 5 km × 15 km, adjacent crustal blocks (Fig. 12). These blocks are limited to the east by the major backthrust of the Nahueve, Neuquén, and Tocomán Rivers. The western boundary of the blocks is less clear, as several thrusts affect them, and the E-W lineaments progressively fade away (Rovere et al., 2004).

Paleomagnetic data indicate a minimum clockwise tectonic rotation of 4.1°, which can be explained by a domino-type pattern of the three crustal blocks delimited by the Trohunco, Lileo, Guañaco, and Reñileuvú Faults (Figure 12b). On the other hand, the northernmost block, limited by the Huaraco and Trohunco Faults, as well as the area to the north of the Río Huaraco, did not rotate since the Early Pleistocene. It is interesting to note that those three blocks correspond to the area with higher tectonic deformation along the ACFS (Folguera et al., 2004) and where the Nahueve-Neuquén-Tocomán backthrust shows a pronounced curve toward the east. Passive rotations of, rigid or non-rigid, in-domino crustal blocks in compressive and transpressional tectonic environments have been shown as an efficient way to accommodate at least a fraction of overall tectonic shortening (Garfunkel, 1989; Nur and Ron, 2003; Zusa and Yin, 2016). In our model, progression of transpressive deformation in the NACFS included the passive clockwise rotation of the aforementioned blocks in Pleistocene times. Our data also suggest that this process was localized in the three blocks south of Trohunco River and did not affect areas to the north. No paleomagnetic data are available for several tens of kilometers to the south of the Reñileuvú Fault, so the southern limits of the tectonic rotations are still unknown, and their definition awaits the obtention of paleomagnetic data in such areas.

The transpressive nature of the NACFS seems to be further confirmed by a clockwise rotation of 25.1° ± 18.3° determined in upper Miocene volcanic rocks exposed in the El Moncol area (some 35 km SW of our study area; Milanese et al., 2023; Fig. 12). This result, together with the small clockwise rotation determined for the area between the Reñileuvú and Trohunco Rivers in the easternmost part of the Guañacos fold and thrust belt in Plio-Pleistocene times supports a model that demonstrates that strike-slip deformation along the ACFS should be taken into

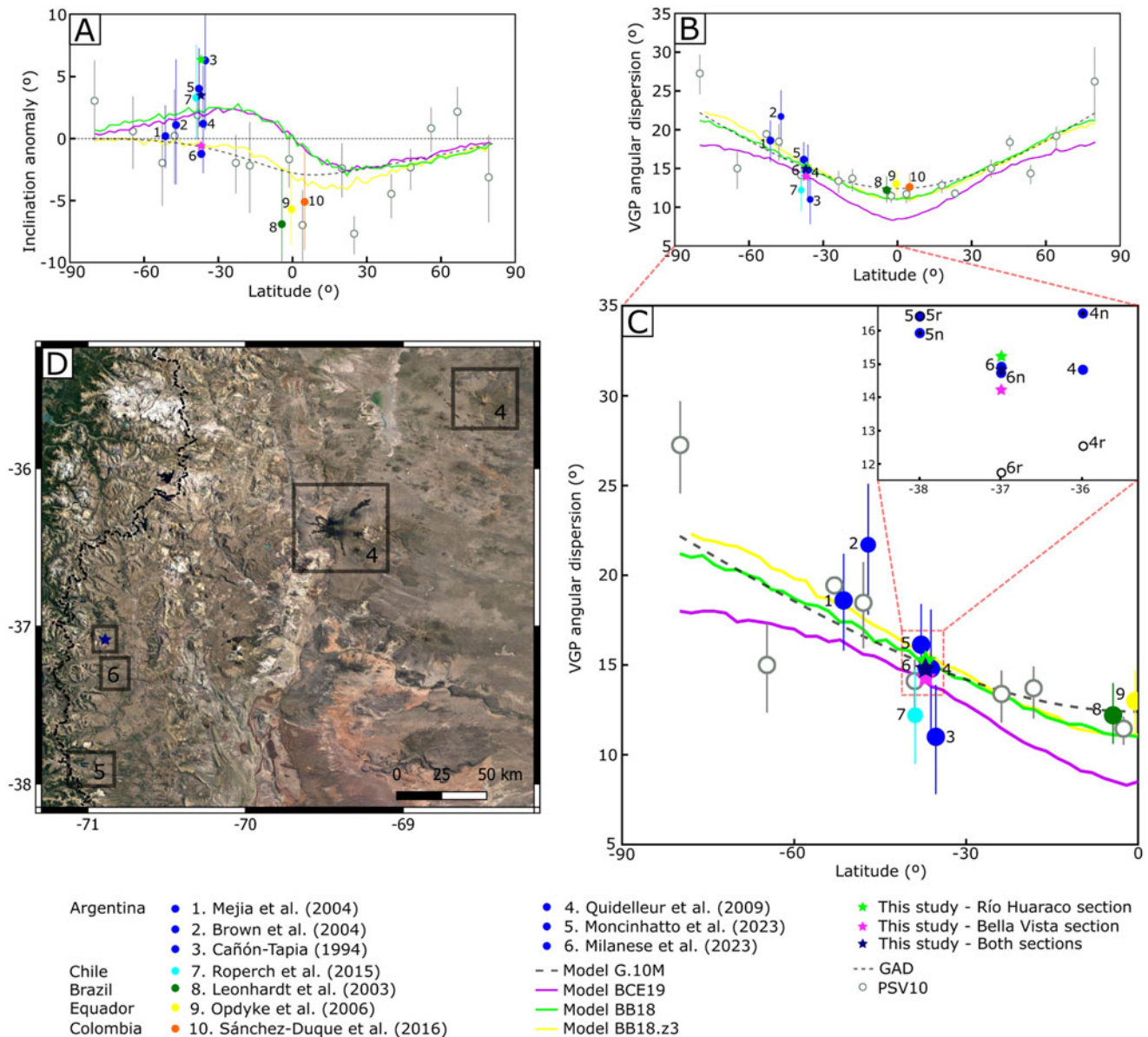


Figure 11. Inclination anomaly (A) and VGP angular dispersion (B) data of different South American paleomagnetic studies. Argentina: Mejia et al. (2004), Brown et al. (2004), Cañón-Tapia (1994), Quidelleur et al. (2009), Moncinhatto et al. (2023), and Milanese et al. (2023); Chile: Roperch et al. (2015); Brazil: Leonhardt et al. (2003); Ecuador: Opdyke et al. (2006); Colombia: Sánchez-Duque et al. (2016). The blue star represents the summary of data from Bella Vista and Río Huaraco sections. (C) The ASD values of this work, corresponding to the normal Gauss chron, and the data of Quidelleur et al. (2009), Moncinhatto et al. (2023), and Milanese et al. (2023), whose normal polarities (black filled circle) correspond to Brunhes and Gauss chrons and the reverse polarities (unfilled circles) to the Matuyama chron. The locations of these studies are in D. Based on Moncinhatto et al. (2023).

account when modeling the Pleistocene structural evolution of this region.

CONCLUSIONS

New paleomagnetic data from Late Pliocene basaltic lavas exposed along two sections in the northern sector of the Neuquén Cordillera (southern Central Andes) suggest normal paleosecular variation during the Gauss normal chron, similar to results found some 80 to 100 km to the south of this area. Anomalous low dispersion of the VGPs in the southern central Andes seems to be limited exclusively to the reverse Matuyama

chron. This behavior of the geomagnetic field in this region should be further studied.

Our and previous paleomagnetic results suggest no significant tectonic rotation of either the Huaraco-Trohunco tectonic block or the areas located north of it. However, the overall mean paleomagnetic direction for the Trohunco-Lileo, Lileo-Guañaco, and Guañaco-Reñieuvú blocks shows a Pleistocene minor clockwise rotation around a vertical axis ($R = 14.4^\circ \pm 10.3^\circ$) interpreted as occurring in a domino-style pattern of such blocks during the Pleistocene.

These and previous results from the nearby area of El Moncol indicate that strike-slip deformation along the ACFZ should be

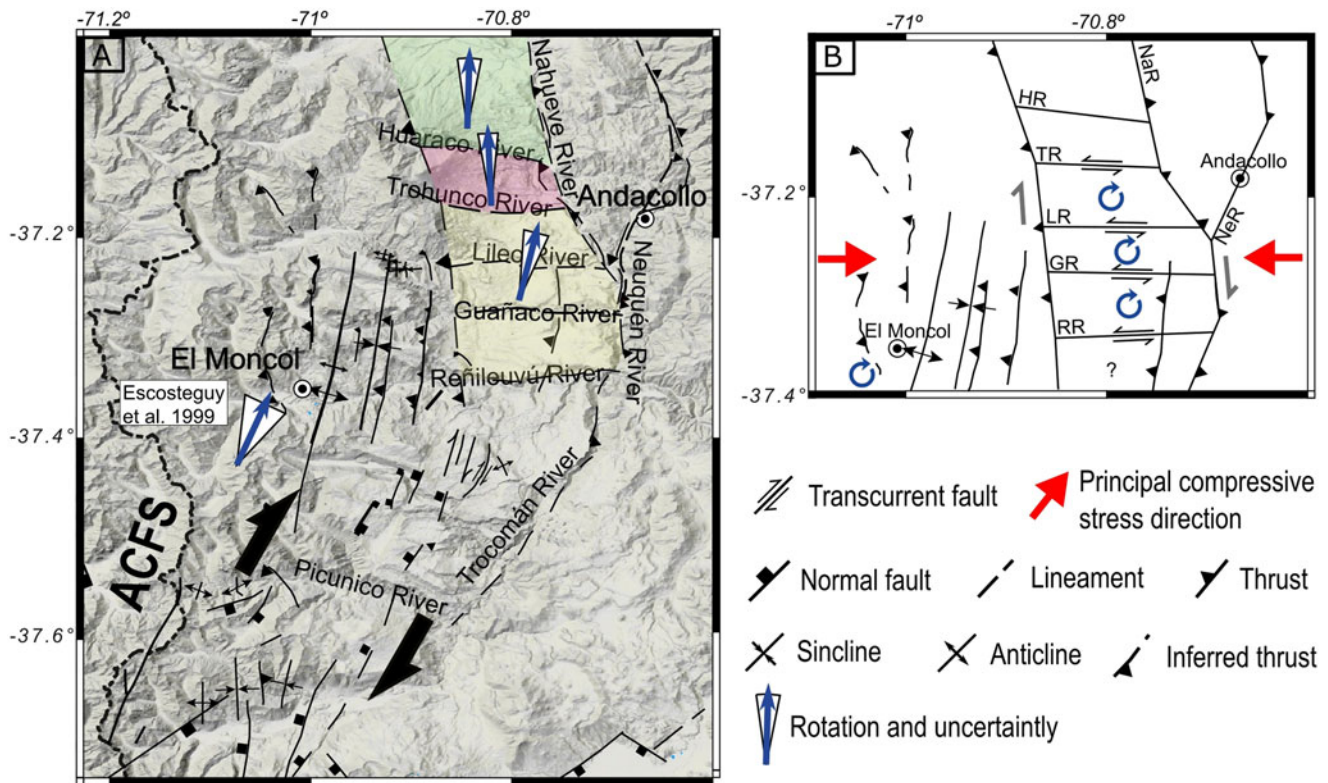


Figure 12. (A) Calculated rotations (R) with their uncertainties for the Bella Vista section (northernmost block), the Huaraco-Trohunco block, and the integrated Trohunco-Lileo, Lileo-Guañaco, and Guañaco-Reñileuvú blocks (Milanese et al., 2023). The clockwise rotation informed by Escosteguy et al. (1999) and recalculated by Milanese et al. (2023) was obtained from upper Miocene volcanic rocks from the Mitrauquén Formation near the El Moncol locality. (B) Simplified tectonic scheme of the northern Antifuerz-Copahue fault zone (NACFZ) with the proposed in-domino clockwise-rotated blocks. HR, Huaraco River; TR, Trohunco River; LR, Lileo River; GR, Guañaco River; RR, Reñileuvú River.

taken into account when modeling the Pleistocene structural evolution of this region.

Acknowledgments. Matías Naselli was extremely helpful with rock magnetic experiments. Thorough and constructive reviews by J. Geissman, an anonymous reviewer, and associate editor J. Urrutia Fucugauchi were extremely useful for improving the earlier versions of the article.

Data Availability Statement. Demagnetization data, isolated paleomagnetic components and mean directions are available at: <https://data.mendeley.com/datasets/fngbxjwgx2/1>.

Financial Support. This study was supported by Consejo Nacional de Investigaciones Científicas y Técnicas (CONICET) via a research grant to A.E.R. (PIP 11220200100476CO) and by the Agencia Nacional de Promoción de la Investigación, el Desarrollo Tecnológico y la Innovación via a research grant to F.N.M. (PICT-2020-01397).

REFERENCES

- Beck, M.E., Jr., 1989. Paleomagnetism of continental North America; implications for displacement of crustal blocks within the Western Cordillera, Baja California to British Columbia. *Geological Society of America Memoirs* **172**, 471–492.
- Beck, M.E., Jr., Burmester, R.F., Cembrano, J., Drake, R., García, A.R., Hervé, F., Munizaga, F., 2000. Paleomagnetism of the North Patagonian batholith, southern Chile. An exercise in shape analysis. *Tectonophysics* **326**, 185–202.
- Bono, R.K., Biggin, A.J., Holme, R., Davies, C.J., Meduri, D.G., Bestard, J., 2020. Covariant giant gaussian process models with improved reproduction

of palaeosecular variation. *Geochemistry, Geophysics, Geosystems* **21**, e2020GC008960.

- Brandt, D., Constable, C., Ernesto, M., 2020. Giant Gaussian process models of geomagnetic paleosecular variation: a directional outlook. *Geophysical Journal International* **22**, 1526–1541.
- Brown, L.L., Singer, B.S., Pickens, J.C., Jicha, B.R., 2004. Paleomagnetic directions and $^{40}\text{Ar}/^{39}\text{Ar}$ ages from the Tatara-San Pedro volcanic complex, Chilean Andes: lava record of a Matuyama-Brunhes precursor? *Journal of Geophysical Research: Solid Earth* **109**(B12). <https://doi.org/10.1029/2004JB003007>.
- Burns, W.M., Jordan, T.E., Copeland, P., Kelley, S.A., 2006. The case for extensional tectonics in the Oligocene-Miocene Southern Andes as recorded in the Cura Mallin basin (36°–38°S). *Special Paper of the Geological Society of America* **407**, 163–184.
- Cañón-Tapia, E., Herrero-Bervera, E., Walker, G., 1994. Flow directions and paleomagnetic study of rocks from the Azufre Volcano, Argentina. *Journal of Geomagnetism and Geoelectricity* **46**, 143–159.
- Cembrano, J., Beck, M.E., Jr., Burmester, R.F., Rojas, C., García, A.R., Hervé, F., 1992. Paleomagnetism of Lower Cretaceous rocks from east of the Lliquiñe-Ofqui fault zone, southern Chile: evidence of small in-situ clockwise rotations. *Earth and Planetary Science Letters* **113**, 539–551.
- Cembrano, J., Hervé, F., 1993. The Lliquiñe Ofqui fault zone: a major Cenozoic strike-slip duplex in the southern Andes. In: *International Symposium on Andean Geodynamics* (No. 2, pp. 175–178), Ed. de l'ORSTOM, Paris.
- Cembrano, J., Hervé, F., Lavenue, A., 1996. The Lliquiñe Ofqui fault zone: a long-lived intra-arc fault system in southern Chile. *Tectonophysics* **259**, 55–66.
- Cembrano, J., Lara, L., 2009. The link between volcanism and tectonics in the southern volcanic zone of the Chilean Andes: a review. *Tectonophysics* **471**, 96–113.

- Cembrano, J., Schermer, E., Lavenue, A., Sanhueza, A., 2000. Contrasting nature of deformation along an intra-arc shear zone, the Liquiñe-Ofqui fault zone, southern Chilean Andes. *Tectonophysics* **319**, 129–149.
- Chadima, M., Cajz, V., Týcová, P., 2009. On the interpretation of normal and inverse magnetic fabric in dikes: examples from the Eger Graben, NW Bohemian Massif. *Tectonophysics* **466**, 47–63.
- Colavitto, B., Sagripanti, L., Jagoe, L., Costa, C., Folguera, A., 2020. Quaternary tectonics in the southern Central Andes (37°–38° S): retroarc compression inferred from morphotectonics and numerical models. *Journal of South American Earth Sciences* **102**, 102697.
- Dearing, J.A., Hay, K.L., Baban, S.M., Huddleston, A.S., Wellington, E.M., Loveland, P., 1996. Magnetic susceptibility of soil: an evaluation of conflicting theories using a national data set. *Geophysical Journal International* **127**, 728–734.
- Demarest, H.H., Jr., 1983. Error analysis for the determination of tectonic rotation from paleomagnetic data. *Journal of Geophysical Research* **88**(B5), 4321–4328.
- de Oliveira, W.P., Hartmann, G.A., Terra-Nova, F., Brandt, D., Biggin, A.J., Engbers, Y.A., Moncinhatto, T.R., 2021. Paleosecular variation and the time-averaged geomagnetic field since 10 ma. *Geochemistry, Geophysics, Geosystems* **22**, e2021GC010063.
- Escosteguy, L.D., Geuna, S.E., Fauqué, L., 1999. La avalancha de rocas del Moncol, Cordillera Principal (Provincia de Neuquén, República Argentina). In: *XIV Congreso Geológico Argentino*. Universidad Nacional de Salta, Salta, pp. 67–70.
- Folguera, A., Ramos, V.A., Díaz, E. F. G., Hermanns, R., 2006. Miocene to Quaternary deformation of the Guañacos fold-and-thrust belt in the Neuquén Andes between 37° S and 37° 30' S. *Geological Society of America Special Paper* **407**, 247–266.
- Folguera, A., Ramos, V.A., Hermanns, R.L., Naranjo, J., 2004. Neotectonics in the foothills of the southernmost central Andes (37°–38° S): evidence of strike-slip displacement along the Antiñir-Copahue fault zone. *Tectonics* **23**, 1–23.
- Folguera, A., Ramos, V.A., Melnick, D., 2003. Recurrencia en el desarrollo de cuencas de intraarco: Cordillera Neuquina (37° 30'–38° S). *Revista de la Asociación Geológica Argentina* **58**, 3–19.
- Folguera, A., Ramos, V.A., Zapata, T., Spagnuolo, M.G., 2007. Andean evolution at the Guañacos and Chos Malal fold and thrust belts (36°–37°S). *Journal of Geodynamics* **44**, 129–148.
- Folguera, A., Rojas Vera, E., Spagnuolo, M., Orts, D., Sagripanti, L., Mariot, M., Ramos, M.E., Bottesi, G., Ramos, V.A., 2011. Los Andes Neuquinos. Geología y Recursos Naturales de la provincia de Neuquén. In: *XVIII Congreso Geológico Argentino*, Relatorio XVIII, pp. 349–354.
- Folguera, A., Yagupsky, D., Melnick, D., 2002. Formación de la Cuenca de Cola de Zorro (5 Ma). Cordillera Neuquina-X Región. Origen y emplazamiento del volcanismo plioceno inferior entre 36° y 39°S. In *Congreso Geológico Argentino* (No. 15).
- García, A.R., Beck, M.E., Jr., Burmester, R.F., Munizaga, F., Hervé, F., 1988. Paleomagnetic reconnaissance of the region de Los Lagos, southern Chile, and its tectonic implications. *Revista Geológica de Chile* **15**, 13–30.
- Garfunkel, Z., 1989. Regional Deformation by Block Translation and Rotation. In: Kissel, C., Laj, C. (Eds.), *Paleomagnetic Rotations and Continental Deformation*. NATO ASI Series, Series C: Mathematical and Physical Science 254. Springer, Dordrecht, Netherlands, pp. 181–208.
- Geissman, J. W., Van der Voo, R., 1980. Thermochemical remanent magnetization in Jurassic silicic volcanics from Nevada, USA. *Earth and Planetary Science Letters* **48**, 385–396.
- González Ferrán, O., Vergara Martínez, M., 1962. *Reconocimiento Geológico de la cordillera de los Andes entre los paralelos 35° y 38°S*. Universidad de Chile, Instituto de Geología, Santiago de Chile.
- Gradstein, F.M., Ogg, J.G., Schmitz, M.D., Ogg, G.M., 2020. *Geologic Time Scale 2020*. Vol. 1. Elsevier, Amsterdam.
- Hernandez-Moreno, C., Speranza, F., Di Chiara, A., 2014. Understanding kinematics of intra-arc transcurrent deformation: paleomagnetic evidence from the Liquiñe-Ofqui fault zone (Chile, 38–41° S). *Tectonics* **33**, 1964–1988.
- Hernandez-Moreno, C., Speranza, F., Di Chiara, A., 2016. Paleomagnetic rotation pattern of the southern Chile fore-arc sliver (38 S–42 S): a new tool to evaluate plate locking along subduction zones. *Journal of Geophysical Research: Solid Earth* **121**, 469–490.
- Hrouda, F., 2011. Models of frequency-dependent susceptibility of rocks and soils revisited and broadened. *Geophysical Journal International* **187**, 1259–1269.
- Jordan, T., Burns, W., Veiga, R., Pángaro, F., Copeland, P., Kelley, S., Mpodozis, C., 2001. Extension and basin formation in the southern Andes caused by increased convergence rate: a mid-Cenozoic trigger for the Andes. *Tectonics* **20**, 308–324.
- Kirschvink, J.L., 1980. The least-squares line and plane and the analysis of paleomagnetic data. *Geophysical Journal International* **62**, 699–718.
- Lange, D., Cembrano, J., Rietbrock, A., Haberland, C., Dahm, T., Bataille, K., 2008. First seismic record for intra-arc strike-slip tectonics along the Liquiñe-Ofqui fault zone at the obliquely convergent plate margin of the southern Andes. *Tectonophysics* **455**, 14–24.
- Leonhardt, R., Matzka, J., Menor, E., 2003. Absolute paleointensities and paleodirections of Miocene and Pliocene lavas from Fernando de Noronha, Brazil. *Physics of the Earth and Planetary Interiors* **139**, 285–303.
- Linares, E., Osters, H.A., Mas, L.C., 1999. Cronología potásio-argón del Complejo Efusivo Copahue-Caviahue, Provincia del Neuquén. *Revista de la Asociación Geológica Argentina* **54**, 240–247.
- Lopez-Escobar, L., Vergara, M., Frey, F.A., 1981. Petrology and geochemistry of lavas from Antuco volcano, a basaltic volcano of the Southern Andes (37° 25'S). *Journal of Volcanology and Geothermal Research* **11**, 329–331, 335–352.
- McFadden, P., Merrill, R., McElhinny, M., 1988. Dipole/quadrupole family modeling of paleosecular variation. *Journal of Geophysical Research: Solid Earth* **93**(B10), 11583–11588.
- Mejia, V., Opdyke, N., Vilas, J., Singer, B., Stoner, J., 2004. Plio-Pleistocene time-averaged field in southern Patagonia recorded in lava flows. *Geochemistry, Geophysics, Geosystems* **5**(3). <https://doi.org/10.1029/2003GC000633>.
- Melnick, D., Rosenau, M., Folguera, A., Echter, H., 2006. Neogene tectonic evolution of the Neuquén Andes western flank (37–39°S). *Geological Society of America Special Paper* **407**, 73–93.
- Milanese, F.N., Rapalini, A.E., Sagripanti, L., Geuna, S., Dekkers, M.J., Feo, R., Folguera, A., 2023. New and revised paleomagnetic data from the southern central Andes: testing tectonic rotations. *Journal of South American Earth Sciences* **124**, 104220.
- Moncinhatto, T.R., de Oliveira, W.P., Haag, M.B., Hartmann, G.A., Savian, J.F., Poletti, W., Trindade, R.I., 2023. Palaeosecular variation in Northern Patagonia recorded by 0–5 Ma Caviahue–Copahue lava flows. *Geophysical Journal International* **234**, 1640–1654.
- Niemeyer, H., Muñoz, J., 1983. Geología de la Hoja Laguna de la Laja, Región del Bío Bío, Escala 1:250.000. Carta N° 57. Servicio Nacional de Geología y Minería de Chile, Santiago.
- Nur, A., Ron, H., 2003. Material and stress rotations: the key to reconciling crustal faulting complexity with rock mechanics. *International Geology Review* **45**, 671–690.
- Opdyke, N.D., Hall, M., Mejia, V., Huang, K., Foster, D.A., 2006. Time averaged field at the equator: results from Ecuador. *Geochemistry, Geophysics, Geosystems* **7**(11). <https://doi.org/10.1029/2005GC001221>.
- Penna, I., 2010. Procesos de remoción en masa en el retroarco norneuquino (37°–38° S): factores condicionantes y sus implicancias en el modelado del paisaje. Doctoral thesis. Universidad de Buenos Aires, Facultad de Ciencias Exactas y Naturales, Buenos Aires.
- Penna, I.M., Hermanns, R.L., Niedermann, S., Folguera, A., 2011. Multiple slope failures associated with neotectonic activity in the Southern Central Andes (37°–37°30'S), Patagonia, Argentina. *GSA Bulletin* **123**, 1880–1895.
- Quiddeleur, X., Carlut, J., Tchilinguirian, P., Germa, A., Gillot, P., 2009. Paleomagnetic directions from mid-latitude sites in the Southern Hemisphere (Argentina): contribution to time averaged field models. *Physics of the Earth and Planetary Interiors* **172**, 199–209.
- Ramos, V.A., Mosquera, A., Folguera, A., García Morabito, E., 2011. Evolución tectónica de los Andes y del Engolfamiento Neuquino adyacente. In: *Geología y Recursos Naturales de la provincia del Neuquén*. Relatorio del XVIII Congreso Geológico Argentino, Buenos Aires, pp. 335–348.

- Rojas, C., Beck, M.E., Jr., Burmester, R. F., Cembrano, J., Hervé, F., 1994. Paleomagnetism of the mid-Tertiary Ayacara Formation, southern Chile: counterclockwise rotation in a dextral shear zone. *Journal of South American Earth Sciences* 7, 45–56.
- Rojas Vera, E., Orts, D.L., Folguera, A., Zamora Valcarce, G., Bottesi, G., Fennell, L., Chiachiarrelli, F., Ramos, V.A., 2016. The transitional zone between the southern central and northern Patagonian Andes (36°–39° S). In: Folguera, A., Naipauer, M., Sagripanti, L., Ghiglione, M.C., Orts, D.L., Giambiagi, L. (Eds.), *Growth of the Southern Andes*. Springer, Cham, Switzerland, pp. 99–114.
- Roperch, P., Chauvin, A., Lara, L. E., Moreno, H., 2015. Secular variation of the Earth's magnetic field and application to paleomagnetic dating of historical lava flows in Chile. *Physics of the Earth and Planetary Interiors* 242, 65–78.
- Rosselot, E.A., Hurley, M., Sagripanti, L., Fennell, L., Iannelli, S.B., Orts, D., Folguera, A., 2020. Tectonics associated with the Late Oligocene to Early Miocene units of the high Andes (Cura-Mallín Formation). A review of the geochronological, thermochronological, and geochemical data. In: Kietzmann, D., Folguera, A. (Eds.), *Opening and Closure of the Neuquén Basin in the Southern Andes*. Springer, Cham, Switzerland, pp. 431–448.
- Rovere, E., Caselli, A., Tourn, S., Leanza, H.A., Hugo, C.A., Folguera, A., Escosteguy, L., et al., 2004. Hoja Geológica 3772-IV, Andacollo, provincia del Neuquén. Boletín 298. Instituto de Geología y Recursos Minerales, Servicio Geológico Minero Argentino, Buenos Aires.
- Sagripanti, L., Colavitto, B., Jagoe, L., Folguera A., Costa, C., 2018. A review about the Quaternary upper-plate deformation in the Southern Central Andes (36–38°S): a plausible interaction between mantle dynamics and tectonics. *Journal of South American Earth Sciences* 87, 221–231.
- Sánchez-Duque, A., Mejía, V., Opdyke, N., Huang, K., Rosales-Rivera, A., 2016. Plio-Pleistocene paleomagnetic secular variation and time-averaged field: Ruiz-Tolima volcanic chain, Colombia. *Geochemistry, Geophysics, Geosystems* 17, 538–549.
- Siravo, G., Speranza, F., Hernandez-Moreno, C., Di Chiara, A., 2020. Orogen-parallel transition from a decoupled fore-arc sliver to Andean-type mountain chain: paleomagnetic and geologic evidence from southern Chile (37–39°S). *Tectonics* 39, e2019TC005881.
- Suárez, M., Emparán, C., 1997. Hoja Curacautín 71, Regiones de la Araucanía y del Bío Bío: escala 1:250.000. Servicio Nacional de Geología y Minería de Chile, Santiago, p. 105.
- Torsvik, T.H., Van der Voo, R., Preeden, U., Mac Niocaill, C., Steinberger, B., Doubrovine, P.V., Cocks, L.R.M., 2012. Phanerozoic polar wander, palaeogeography and dynamics. *Earth-Science Reviews* 114, 325–368.
- Vergara Martínez, M., Muñoz Bravo, J., 1982. La Formación Cola de Zorro en la alta Cordillera Andina Chilena (36°-39°Lat. S), sus características petrográficas y petrológicas: una revisión. *Revista Geológica de Chile* 17, 31–46.
- Watson, G.S., 1956. A test for randomness of directions. *Geophysical Supplements to the Monthly Notices of the Royal Astronomical Society* 7, 160–161.
- Zijderveld, J.D.A., 1967. A. C. demagnetization of rocks: analysis of results. In: Collinson, D.W., Creer, K.M., Runcorn, S.K. (Eds.), *Methods in Palaeomagnetism*. Elsevier, Amsterdam, pp. 254–286. <https://doi.org/10.1016/b978-1-4832-2894-5.50049-5>.
- Zuza, A.V., Yin, A., 2016. Continental deformation accommodated by non-rigid passive bookshelf faulting: an example from the Cenozoic tectonic development of northern Tibet. *Tectonophysics* 677, 227–240.